Piecing together the Ganges-Brahmaputra-Meghna River delta: Use of sediment provenance to reconstruct the history and interaction of multiple fluvial systems during Holocene delta evolution

Steven L. Goodbred Jr.[1,†], Penny M. Paolo[2], Mohammad Shahid Ullah[1], Russell D. Pate[1], Sirajur R. Khan[3], Steven A. Kuehl[4], Sunil K. Singh[5], and Waliur Rahaman[5]

[1]*Department of Earth and Environmental Sciences, Vanderbilt University, Nashville, Tennessee 37240, USA*
[2]*School of Marine and Atmospheric Sciences, Stony Brook University, Stony Brook, New York 11794, USA*
[3]*Geological Survey of Bangladesh, Ministry of Power, Energy and Mineral Resources, Segunbagicha, Dhaka 1000, Bangladesh*
[4]*Virginia Institute of Marine Science, College of William and Mary, Gloucester Point, Virginia 23062, USA*
[5]*Geosciences Division, Physical Research Laboratory, Navrangpura, Ahmedabad, Gujarat 380009, India*

ABSTRACT

Three main rivers—the Ganges, Brahmaputra, and Meghna—coalesce in the Bengal basin to form the world's largest delta system, which serves as filter and gateway between the Himalayan collision and vast Bengal fan repository. New insights into the Holocene construction of the Ganges-Brahmaputra-Meghna delta, with a focus on river sedimentation, channel migration, and avulsion history, are presented here using the Sr geochemistry of bulk sediments as a provenance tracer. The sediment load of each river transmits a distinct Sr signature owing to differences in source rocks from the Himalaya, Tibet, and local regions, allowing for effective tracking of river channels and stratigraphic development within the delta. In the early Holocene, vigorous delta aggradation occurred under rapid sea-level rise and high river discharge and supported the construction of sand-dominated stratigraphy by laterally mobile, braided-stream channels. However, the vertically (i.e., temporally) uniform, but geographically distinct, Sr signatures from these deposits indicate that the Ganges, Brahmaputra, and Meghna fluvial systems remained isolated from one another and apparently constrained within their lowstand valleys. By the mid-Holocene, though, delta stratigraphy records spatially and temporally nonuniform Sr signatures that hallmark the onset of avulsions and unconstrained channel migration, like those that characterize the modern Ganges and Brahmaputra fluvial systems. Such mobility developed in the mid-Holocene despite declining discharge and sea-level rise, suggesting that earlier channel behavior had been strongly influenced by antecedent topography of the lowstand valleys. It is only after the delta had aggraded above the valley margins that the fluvial systems were able to avulse freely, resulting in numerous channel reorganizations from mid-Holocene to present. These channel-system behaviors and their role in delta evolution remain coarsely defined based only on this initial application of Sr-based provenance tools, but the approach is promising and suggests that a more complete understanding can be achieved with continued study.

INTRODUCTION

Most sediment eroded from continental basins is dispersed to the oceans through narrow fluviodeltaic gateways, where sediment loads are filtered and transformed, and 20%–80% of the sediment load is generally sequestered within the delta before reaching the continental slope (e.g., Goodbred and Kuehl, 1999; Nittrouer et al., 2007; Walsh et al., 2014). Thus, deltas play a major role in defining the mass and character of terrigenous sediment that is discharged to the ocean and that constitutes the long-term geologic record. Among the world's largest sediment dispersal systems, the Ganges and Brahmaputra Rivers of South Asia drain approximately two thirds of the Himalayan orogen and together deliver >1 Gt/yr of sediment to the Bengal margin, where they construct and sustain the world's largest delta and marine fan system (Fig. 1; Curray and Moore, 1971; Kuehl et al., 2005). Along this transport pathway, at least two thirds of the riverine sediment load has been trapped within the delta through the Holocene, constructing 50–90 m of stratigraphy that preserves a high-resolution record of fluviodeltaic processes and regional environmental change (Goodbred and Kuehl, 1999; Goodbred, 2003).

Over the Holocene, the three main Ganges-Brahmaputra-Meghna delta rivers have deposited ~8500 km^3 of sediment within the Bengal basin (Goodbred and Kuehl, 2000b), but the sediment load of each river is also geochemically distinct, making this an ideal location to unravel the history of multiple fluvial systems interacting within a tectonically active basin to construct a major deltaic sequence. Such information is directly relevant to the 150 million people living on the Ganges-Brahmaputra-Meghna delta, where understanding patterns and controls of river behavior and delta sedimentation is essential to anticipating impacts of relative sea-level rise, climate variability, and shifts in land use and water management (e.g., Nicholls and Goodbred, 2005; Woodroffe et al., 2006; Brammer, 2014). Furthermore, the source, depositional history, and stratigraphic architecture of Ganges-Brahmaputra-Meghna delta sediments are known to be key controls on the behavior of groundwater arsenic, which is widespread but heterogeneously distributed within Holocene aquifers of the delta (e.g., Aziz et al., 2008; McArthur et al., 2008; Weinman et al., 2008).

Within the Himalayan orogen and surrounding geologic terranes, strontium (Sr) isotopes have become a well-established provenance tracer for source rocks, and they are often used in conjunction with Nd isotopes to unravel patterns of erosion and sediment dispersal within the region (e.g., Derry and France-Lanord,

†E-mail: steven.goodbred@vanderbilt.edu.

GSA Bulletin; doi: 10.1130/B30965.1; 9 figures; Data Repository item 2014225.

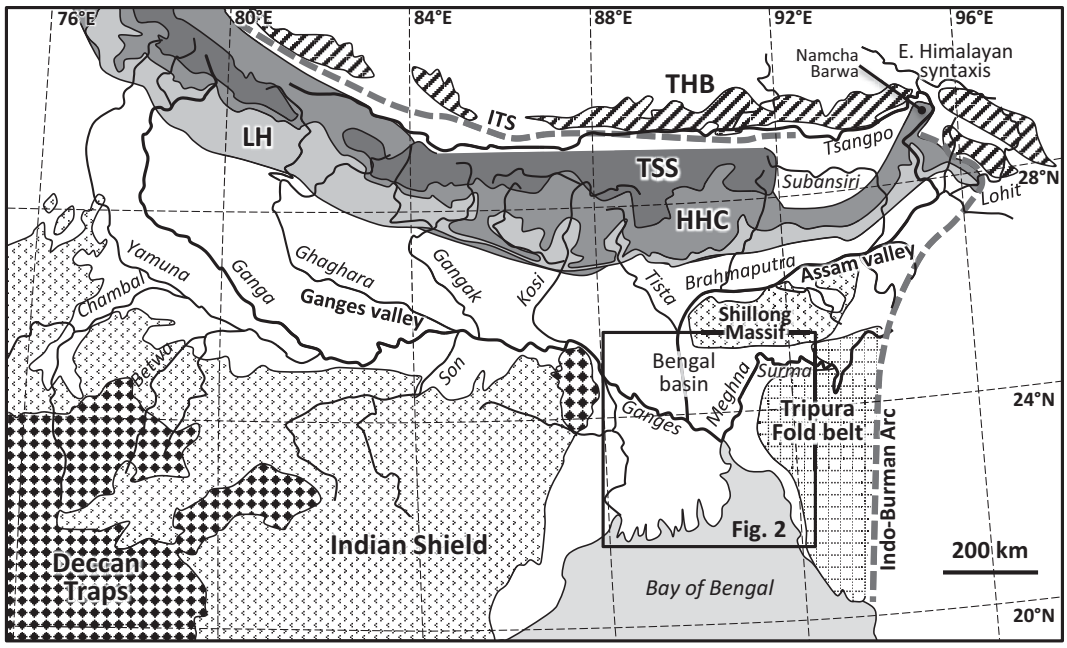

Figure 1. Map of major tributaries and source rocks contributing sediment to the Bengal basin and Ganges-Brahmaputra-Meghna River delta, including the Trans-Himalayan batholiths (THB), Tethyan Sedimentary Series (TSS), High Himalayan Crystalline Sequence (HHC), and Lesser Himalayas (LH). The Deccan Traps and Indian Shield contribute relatively little sediment. The Shillong Massif and Tripura fold belt are locally important sediment sources to the eastern Bengal basin. ITS—Indus-Tsangpo suture. (Figure redrawn after Galy et al., 2010.)

1996; Galy et al., 1996; Galy and France-Lanord, 2001; Singh and France-Lanord, 2002; Najman, 2006; Singh et al., 2006, 2008; Rahaman et al., 2009). Here, we present the first Sr isotope measurements, and some Nd isotope measurements, for Holocene stratigraphy of the Ganges-Brahmaputra-Meghna delta. In addition, measurements of bulk-sediment Sr concentrations are also introduced as an effective first-order provenance marker and are shown to be a valuable proxy in conjunction with Sr and Nd isotopes. Together, results from these provenance indicators provide a more thorough understanding of Holocene delta evolution and river course changes than have been otherwise possible using grain size and sedimentological measurements alone.

BACKGROUND

Bengal Basin

The Ganges-Brahmaputra-Meghna delta has formed within the Bengal basin along the trailing-edge margin of the Indian plate at its juncture with the Eurasian and Sunda plates (Steckler et al., 2008). Along the basin's northeast border, it is being overthrust by the Shillong Massif along the steeply dipping Dauki fault (Fig. 2). The Bengal basin is also shortening to the east along the Indo-Burman Arc, where the Tripura fold belt is actively growing and overthrusting the delta (Steckler et al., 2008). The high topography that is developing along these deformation fronts receives high precipitation as well, combining to yield locally important sediment sources that have contributed to construction of the Ganges-Brahmaputra-Meghna delta (Pickering et al., 2013).

Within the Bengal basin itself, elevated Pleistocene sediments, notably the Madhupur terrace and Barind tracts, serve as topographic barriers that influence river migration and sediment dispersal (Fig. 2; Goodbred et al., 2003; Pickering et al., 2013). This partitioning of Bengal basin and its underlying tectonic controls support varying rates of subsidence across the Ganges-Brahmaputra-Meghna delta, from millennial-scale rates of 1–3 mm/yr in the southern regions to 4 mm/yr or more in the northeast Sylhet basin (Goodbred and Kuehl, 2000a; Hanebuth et al., 2013). During the Holocene, accommodation produced through subsidence and glacioeustatic sea-level rise has led to development of thick fluvial and coastal marine deposits that reach 70–90 m depth within the lowstand valleys and central Sylhet basin (Umitsu, 1993; Goodbred and Kuehl, 2000a). Broad interfluves that separate the lowstand valleys are defined by a well-developed paleosol that dips southward from outcrop exposures to ~50 m below surface, buried by Holocene delta sediments (Goodbred and Kuehl, 2000a; McArthur et al., 2008; Sarkar et al., 2009).

Ganges and Brahmaputra River Catchments

Sediments delivered by the Ganges and Brahmaputra Rivers derive primarily from the Himalayan orogeny, with minor inputs from the Indian craton (Galy and France-Lanord, 2001; Singh and France-Lanord, 2002; Wasson, 2003; Garzanti et al., 2004; Sinha et al., 2005; Singh et al., 2007). The principal source rocks include the Trans-Himalayan batholiths, Tethyan Sedimentary Series, High Himalayan Crystalline Sequence, and Lesser Himalayas (Fig. 1). The Tethyan Sedimentary Series and High Himalayan Crystalline Sequence comprise the dominant rock units exposed along the peaks and drainage divide of the Himalaya, with the Tethyan Sedimentary Series exposed primarily along the back slope, and the High Himalaya Crystalline Sequence along the wetter, more rapidly eroding front slope. As such, High Himalayan exposures mostly drain southward to the Ganges watershed, whereas the Tethyan rocks principally drain north into the Brahmaputra catchment (Fig. 1). Unlike the Tethyan and High Himalayan series, the monzonitic Trans-Himalayan batholiths are exclusive to the Brahmaputra watershed and are widely exposed along the Indus-Tsangpo suture and around the eastern Himalayan syntaxis (Fig. 1). Low-grade sedimentary rocks of the Lesser Himalaya are well exposed within the Ganges' watershed, but in the Brahmaputra catchment, they outcrop only locally along Assam Valley tributaries. For each of these source rocks, their mineralogical and isotopic characteristics are well preserved in the sediments that they contribute to the mainstem rivers (Richards et al., 2006), allowing for the relative contribution of each source to be calculated for the Ganges and Brahmaputra sediment loads (e.g., Singh and France-Lanord, 2002; Singh et al., 2008; Garzanti et al., 2010, 2011; Lupker et al., 2012).

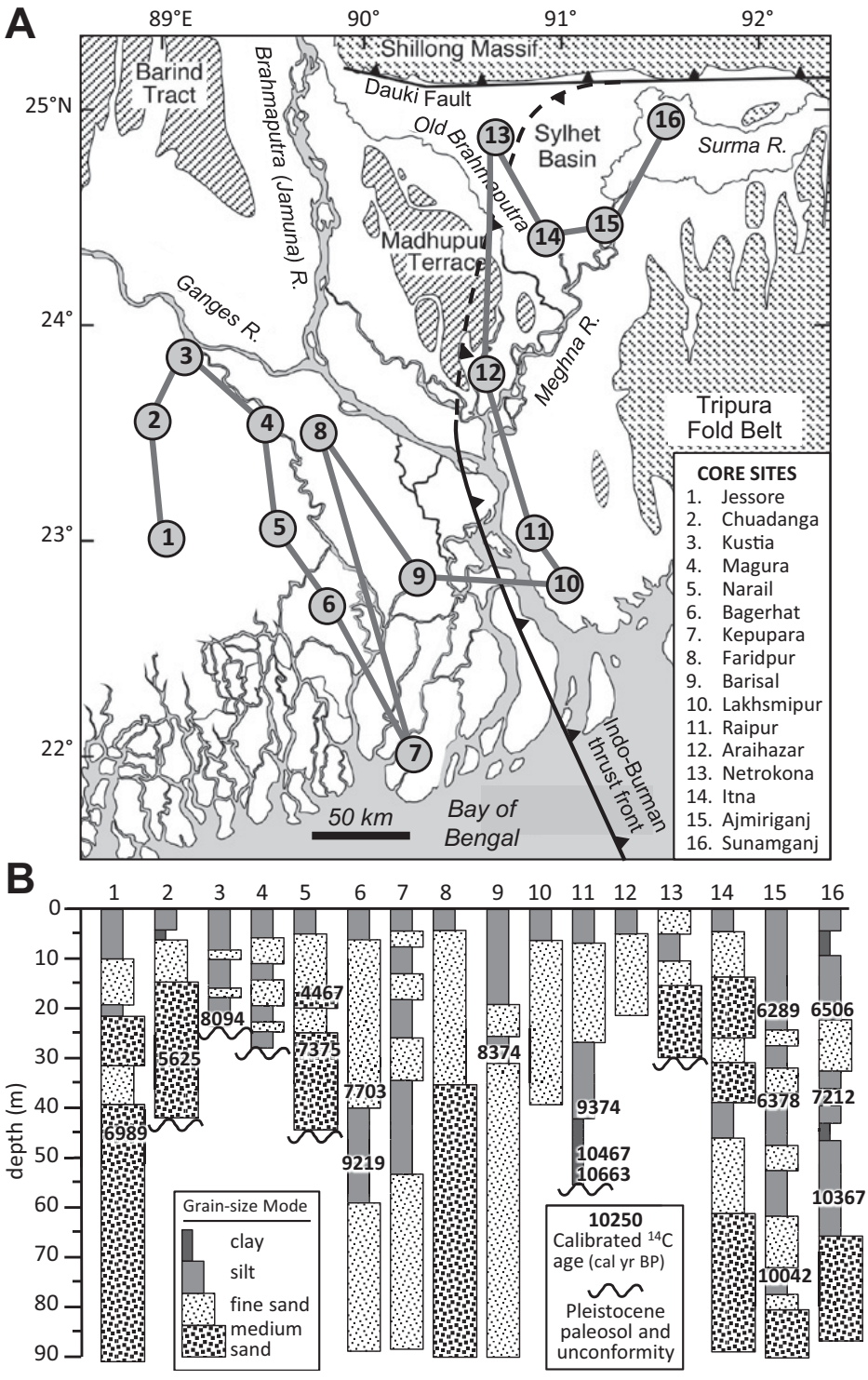

Figure 2. (A) Map of the Bengal basin and Ganges-Brahmaputra-Meghna River delta with location of cores used in this study. (B) Summary of Holocene stratigraphy and radiocarbon ages for cores shown in A. Subsurface stratigraphy for most of the basin is dominated by fine to medium sands deposited by the main rivers, with shallow stratigraphy (0–10 m depth) comprising primarily silty overbank floodplain deposits. Older floodplain muds within the subsurface are locally preserved away from the central river valleys, such as cores 1, 3, 4, 13, and 14. Thicker mud units (15–25 m thick) are preferentially preserved within the tidal delta plain (cores 6, 7, 9, and 11) and the tectonically subsiding Sylhet basin (cores 15 and 16).

The Ganges headwaters originate along the Tibetan border in north India, with the full watershed draining large areas of the Himalayan front slope and Indian craton (Fig. 1). At its entry point to the Bengal basin, the Ganges load consists of 90% ± 5% Himalayan-derived sediment, principally from the High Himalayan Crystalline sources (65% ± 10%; Wasson, 2003; Singh et al., 2008; Lupker et al., 2012). As is the case throughout the Himalayas, the Ganges catchment is characterized by significant spatial variability in longer-term erosional fluxes (>10^3 yr; e.g., Thiede et al., 2009; Lupker et al., 2012; Blöthe and Korup, 2013). However, investigations of modern erosion suggest that rates are more comparable when normalized to basin size and sediment discharge, suggesting that these disparate basins exhibit relatively similar erosion behavior (Andermann et al., 2012). Lupker et al. (2012) also noted that the chemical composition of modern noncarbonate sediments from Himalayan-front tributaries is "remarkably homogeneous." Although spatiotemporal variations in erosion remain imprecise for the Ganges basin, the integrated load from the watershed is reasonably well constrained to 400 ± 50 × 10^6 tons of sediment delivered to the Bengal basin annually (Milliman and Syvitski, 1992; Lupker et al., 2011).

Draining the back slope of the Himalaya, the Brahmaputra River originates in Tibet, where the stream is known as the Tsangpo (Fig. 1). The Tsangpo channel tracks the continental suture between India and Asia, draining the geochemically distinct monzonites of the Trans-Himalayan batholiths (Schärer et al., 1984; Debon et al., 1986). The Tsangpo ultimately traverses the Himalayas via the Namcha Barwa syntaxis. There, the channel steeply drops 2 km in elevation (gradient = 0.02) where rapid bedrock incision is sustained along the thermally coupled "tectonic aneurysm" (i.e., thinned crust) of the syntaxis (Zeitler et al., 2001; Finnegan et al., 2008). Although the syntaxis encompasses just 4% of the Brahmaputra's catchment area, various studies calculate the region to contribute as much as 45% ± 15% of the sediment load (Singh and France-Lanord, 2002; Garzanti et al., 2004; Stewart et al., 2008). Below the syntaxis, the Brahmaputra debouches into the low-lying Assam Valley and Himalayan foreland, where most of the remaining load is contributed by Himalayan tributaries having a dominant High Himalayan Crystalline lithology (Fig. 1). Entering the Bengal basin and Ganges-Brahmaputra-Meghna delta, the modern Brahmaputra delivers 600 ± 50 × 10^6 tons of sediment annually (Coleman, 1969; Milliman and Syvitski, 1992; Wasson, 2003).

Strontium Geochemistry of Ganges-Brahmaputra Fluvial Sediment

The dominance of High Himalayan erosion in the Ganges catchment is responsible for the relatively radiogenic $^{87}Sr/^{86}Sr$ (0.758–0.788) and relatively low $[Sr]_{sil}$ value (79–92 ppm) of its sediment load at the Bengal basin (Galy and France-Lanord, 2001; Singh et al., 2008). For the Brahmaputra, major sediment contributions from the syntaxis and exposures of the Trans-Himalayan batholiths yield a less-radiogenic $^{87}Sr/^{86}Sr$ signature with values of 0.716–0.735 and considerably higher Sr concentrations of 148–183 ppm (Galy and France-Lanord, 2001; Singh and France-Lanord, 2002). More recent data for Ganges and Brahmaputra sediment collected within the delta reveal that $^{87}Sr/^{86}Sr$ is considerably higher in suspended material than in the bed load (Lupker et al., 2013). Detailed results yield $^{87}Sr/^{86}Sr$ values of 0.758–0.769 for Ganges bed load compared with 0.766–0.802 for its suspended load. In the Brahmaputra system, $^{87}Sr/^{86}Sr$ values exhibit a similar difference between bed load and suspended load, with ranges of 0.721–0.728 and 0.725–0.755, respectively (Singh and France-Lanord, 2002; Lupker et al., 2013).

With regard to the concentration of Sr in these regional source rocks, Sr is almost exclusively associated with calcium-bearing minerals, where it readily substitutes for Ca due to its similar charge and ionic radius (Faure and Powell, 1972). The principal Ca-bearing minerals found in detrital sediments of the region include plagioclase feldspar (e.g., anorthite), carbonates (e.g., calcite, dolomite), the heavy mineral epidote, and secondary contributions from apatite and phyllosilicates (e.g., biotite). In general, Sr-enriched plagioclase feldspars are more abundant in plutonic and meta-igneous rocks, particularly the feldspathic Trans-Himalayan batholiths (e.g., Garzanti et al., 2004, 2010). Indeed Garzanti et al. (2010), in their detailed geochemical evaluation of Ganges-Brahmaputra sands, calculated that 75%–80% of Sr transported by the two rivers is associated with feldspars and lithic fragments (the latter presumed rich in feldspar; GSA Data Repository Fig. S1[1]). Of the remaining Sr fraction, 20%–25% is contributed by epidote (8%–20%), with minor contributions (<5%) from phyllosilicates, amphiboles, and apatites (Garzanti et al., 2010). These minerals, however, encompass a considerable range of density, weatherability, and source-rock associations, requiring that any application of Sr concentration as a provenance indicator consider these potential influences (see Results section).

METHODS

This study presents a compilation of samples and data from several research projects. As a result, there are some minor differences in analytical techniques based on the specific resources available at the participating institutions, which are described next. However, the same sample-preparation methods were employed, and the geochemical analyses were each held to the same standards for error and reproducibility, allowing for comparable data sets.

Boreholes 1–3, 5, 7, and 12 were collected using a hand-drilled reverse-circulation method that is locally used for tubewell installation, with samples taken from cuttings at 1.5 m intervals. The remaining boreholes were collected using a hollow-stem auger with a split-spoon sampler and sediments collected at 1.5 m intervals (Goodbred and Kuehl, 2000a; Pate et al., 2009). In preparation for chemical analyses, 30–50 g aliquots of bulk sediment were ashed at 600 °C for 48 h to remove organic material and destabilize refractory carbonates. Carbonates were then leached from the combusted samples using 15% acetic acid on a hot plate at 80 °C. This method does not necessarily ensure complete carbonate removal, but results are compared with published data to ensure that there were no significant effects of residual carbonates (Fig. S2 [see footnote 1]). The leached, combusted samples were then thoroughly rinsed and dried before they were crushed to a fine powder using a Shatterbox mill. Grain-size distributions were measured on unaltered sediments using either (1) a settling tube and pipette analysis for the sand and finer fractions, respectively, or (2) a Malvern Mastersizer 2000E laser-diffraction particle-size analyzer. Radiocarbon ages are presented here as calibrated sidereal years (cal. yr B.P.), and all data have been previously published (Goodbred and Kuehl, 2000a).

Prepared samples were analyzed for major- and trace-element concentrations (n = 120) at either Washington State University GeoAnalytical Laboratory using X-ray fluorescence (XRF) and inductively coupled plasma–mass spectrometry (ICP-MS) or at Middle Tennessee State University using XRF following standard procedures (Tables S1 and S2 [see footnote 1]). Blind duplicates were analyzed with each sample set for quality assurance. Additional Sr concentration measurements were gathered at City University of New York Queens College in Queens, New York, using an Innov-X Alpha handheld XRF. Samples were analyzed in duplicate and periodically normalized to three different standards: NIST 1646a, USGS BCR-2, and USGS GSP-2. The accepted error for measurements from each of the three techniques was less than ±5ppm for Sr.

Sr and Nd isotope measurements were performed at either the Isotope Laboratory at Stony Brook University in Stony Brook, New York, or at the Physical Research Laboratory in Ahmedabad, India (Table S2 [see footnote 1]). For $^{87}Sr/^{86}Sr$ analysis (n = 89) at Stony Brook University, a 50 mg portion of prepared sample was weighed into 7 mL Savillex® Teflon vials and dissolved via a series of acid digestions utilizing HF, HNO_3, and HCl. Sr was separated using SrSPEC® resin and then loaded onto outgassed W filaments for analysis on a Finnigan MAT 262 multicollector–thermal ionization mass spectrometer (TIMS) in dynamic mode. Similar digestion procedures were followed at the Physical Research Laboratory, where Sr isotopes were measured using an Isoprobe–T TIMS, and Nd isotopes (n = 20) were measured using a Finnigan Neptune MC-ICP-MS and the MC-321 standard. The $^{87}Sr/^{86}Sr$ values at both laboratories were normalized to $^{86}Sr/^{88}Sr$ of 0.1194 using the standard SRM 987, with precision of <0.000025 2σ. Internal reproducibility for both Sr and Nd isotopes was less than 10 ppm (1σ). At both locations, blank measurements were taken but found to be at concentrations several orders of magnitude less than sample concentrations; therefore, no corrections were required.

RESULTS

Based on previous investigations of Ganges and Brahmaputra sediment geochemistry and mineralogy (e.g., Singh and France-Lanord, 2002; Singh et al., 2008; Garzanti et al., 2010, 2011), we initially disaggregated our Bengal basin data set into low-Sr, medium-Sr, and high-Sr groups according to their $[Sr]_{sil}$ values (Figs. 3 and 4). For this study, low-Sr samples are considered to be those having $[Sr]_{sil}$ <100 ppm, a range that is consistent with previous results for modern Ganges sediment (Singh et al., 2008). The high-Sr samples are defined as those with $[Sr]_{sil} \geq 140$ ppm, which corresponds to the range for typical Brahmaputra sediment (Singh and France-Lanord, 2002). The difference in Sr concentrations between the two rivers is controlled primarily by mineralogy and explained by the 2–3-fold higher abundance of Sr-bearing plagioclase feldspars in Brahmaputra sediments versus those of the Ganges (Fig. S1B [see footnote 1]; Garzanti et al., 2010). The medium-Sr samples, ranging 100–140 ppm $[Sr]_{sil}$, are not

[1]GSA Data Repository item 2014225, supplementary figures and data tables, is available at http://www.geosociety.org/pubs/ft2014.htm or by request to editing@geosociety.org.

coincident with the main-stem river values, which at least initially suggests that they reflect a mixed sediment source. Here, we do not a priori ascribe the Bengal basin sediments to a particular river system, but we establish these initial ranges to assess the overall characteristics and spatial distributions of the aggregate data set. Note that the use of "high-Sr" and "low-Sr" are relative valuations, as the Sr concentration of all Bengal basin sediment is considerably depleted compared with the mean value of 360 ppm for upper continental crust (UCC) composition (Rudnick and Gao, 2003).

Strontium Geochemistry

Grain-Size Effects

The mean grain size of fluvial sediment typically decreases downstream due to physical and chemical weathering during transport. Thus, grain size is a common control on bulk-sediment geochemistry, with the concentration of more conservative elements (e.g., TiO_2, Al_2O_3) generally negatively correlated with grain size. This relationship is largely defined by the preferential loss of unstable silicates and mobile elements through weathering and the corresponding enrichment of more alumina-bearing minerals such as pedogenic clays (McLennan et al., 2003). Here, we evaluate Sr concentrations relative to the ratio of alumina to silica (Al_2O_3/SiO_2) as a geochemical proxy for grain size (e.g., Galy et al., 2008). This relationship shows no correlation of $[Sr]_{sil}$ with Al_2O_3/SiO_2 for either the bulk data set or within the individual high-Sr, medium-Sr, and low-Sr groups (Fig. 3A). The lack of correlation also holds when $[Sr]_{sil}$ is compared with TiO_2, another conservative element that negatively correlates with grain size (Fig. 3B). These findings are comparable with other data sets from the region that similarly show no systematic relationship between grain size and bulk-sediment Sr concentrations (e.g., Garzanti et al., 2010; Lupker et al., 2013). The conclusion for this data set is that grain-size variations play a secondary role in bulk-sediment Sr concentrations and thus do not overwhelm the source-rock difference between Ganges- and Brahmaputra-derived river sediments. Such a result should not be assumed for other data sets, for which the relationship of grain size and Sr concentration should be independently tested.

Weathering Effects

The degree of weathering that sediments have experienced can also affect bulk-element concentrations. A general approach often used to assess the weathering loss of feldspar-group minerals is the chemical index of alteration (CIA), which considers the preferential loss of major oxides relative to more refractory alumina (Nesbitt and Young, 1982; Nesbitt et al., 1996). The CIA is represented as,

$$CIA = [Al_2O_3/(Al_2O_3 + CaO^* + Na_2O + K_2O)] \times 100,$$

with each term expressed in molar weight percent, and the CaO* term representing calcium associated with the silicate fraction only to avoid bias from carbonates (Fedo et al., 1995). For unweathered granitic rocks, typical CIA values are 45–55, with similar values of ~50 for fresh feldspars (Nesbitt and Young, 1982). Values increase considerably to 75–90 for illite, a common clay product of feldspar weathering (McLennan, 1993). Given the dominantly felsic composition of Ganges-Brahmaputra sediments (Garzanti et al., 2004, 2010, 2011), the CIA values of 50–65 calculated for the present data set places them in the range of unaltered to modestly altered sediments (McLennan, 1993). Overall, these values indicate that the geochemical composition of Holocene silicate sediments in the Bengal basin has not been significantly altered by weathering. However, the precision of this tool for detecting differences in the weathering intensity of Ganges-Brahmaputra-Meghna delta sediments is limited because the initial source-rock mineralogy is different for the three main river catchments (Fig. 1).

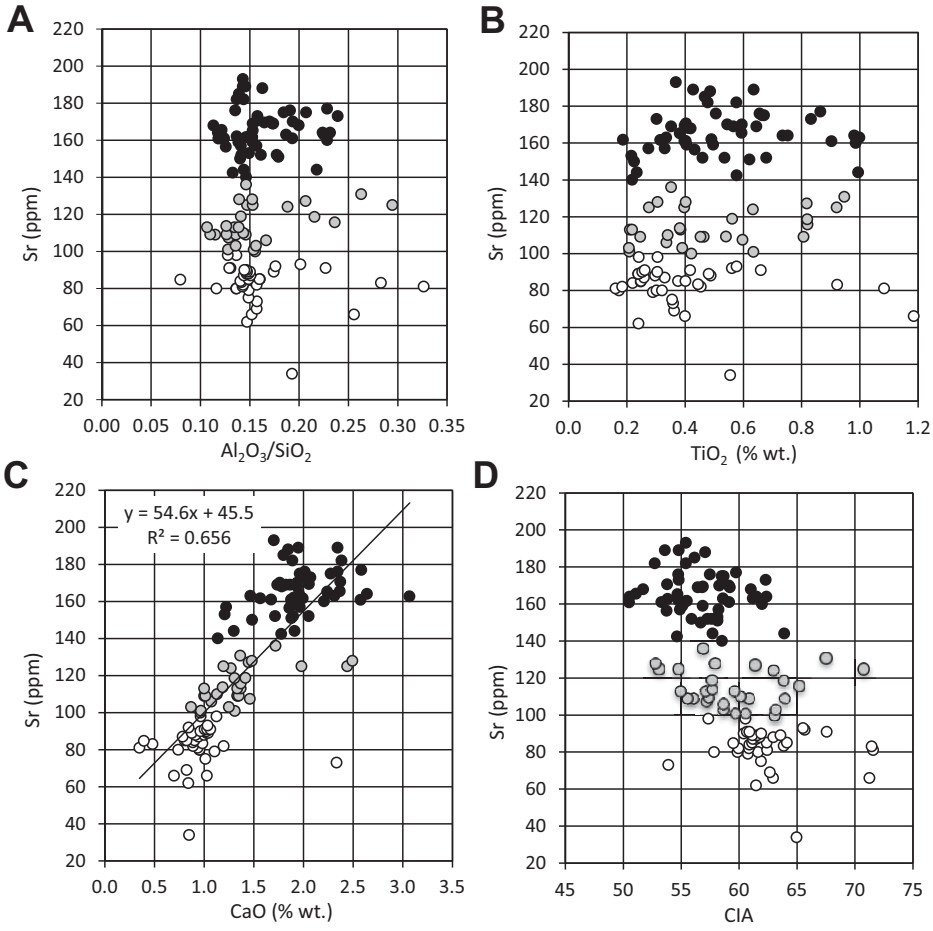

Figure 3. Scatter plots of silicate [Sr] relative to (A) Al_2O_3/SiO_2, (B) TiO_2, (C) CaO, and (D) the chemical index of alteration (CIA). Al_2O_3/SiO_2 and TiO_2 can be taken as general proxies for sediment grain size but here show no relationship with [Sr]. (C) In contrast, Sr covaries with CaO, for which it substitutes in Ca-bearing minerals, primarily plagioclase feldspars. (D) Weathering is another potential control on Sr concentrations, and here [Sr] shows a slight negative trend with CIA due to differences in the initial concentration of CaO in regional source rocks, not the degree of sediment weathering. Note the black, gray, and white-keyed data points correspond with the high-Sr, medium-Sr, and low-Sr groups defined and discussed in the text.

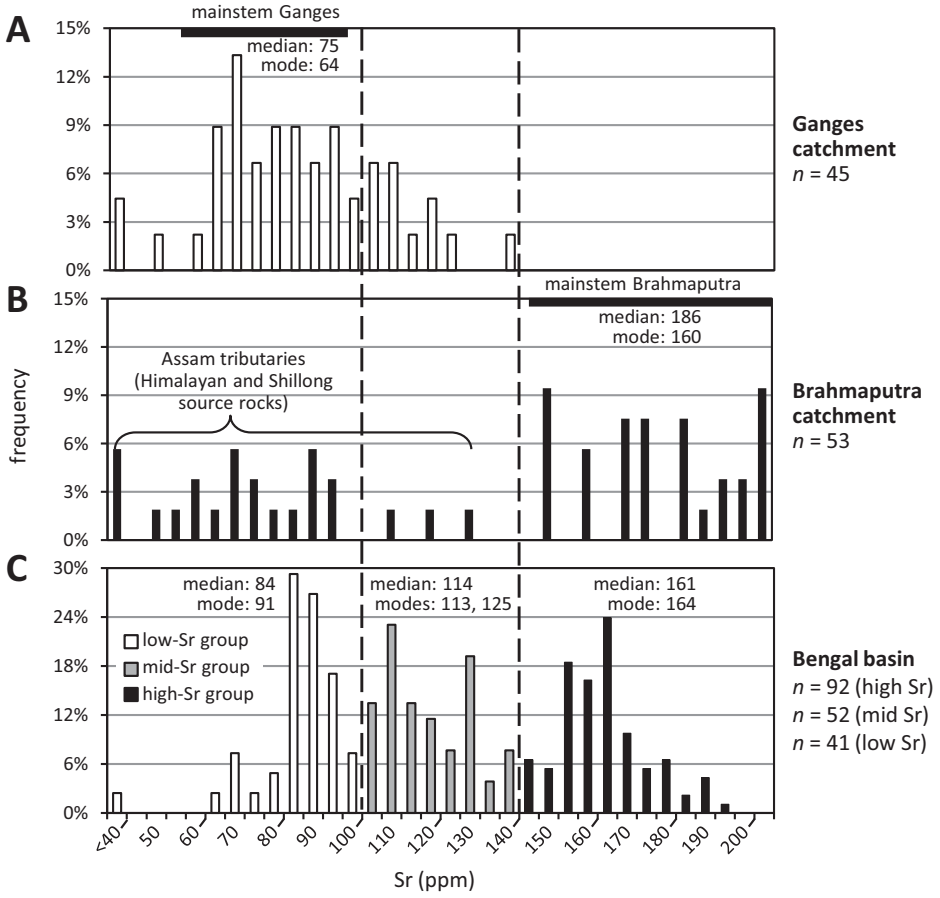

Figure 4. Histograms of silicate [Sr] from fluvial sediments in (A) the Ganges River catchment (Singh et al., 2008), (B) the Brahmaputra River catchment (Singh and France-Lanord, 2002), and (C) the Bengal basin (this study). Black bars in A and B show the range of $[Sr]_{sil}$ values for sediment within the main-stem channel of each river, with values outside of this range representing sediment from specific tributaries. The range of $[Sr]_{sil}$ values for the main-stem Ganges and Brahmaputra each defines distinct sediment populations. (C) Results from the Bengal basin exhibit modes that correspond to Ganges and Brahmaputra end-member sediments, as well as two intermediate modes reflecting populations of mixed-source sediments.

Although the CIA values suggest that Ganges-Brahmaputra-Meghna delta sediments are relatively unaltered, weathering intensity may have varied with the significant climatic and hydrological changes that have occurred across South Asia during the Holocene (e.g., Goodbred and Kuehl, 2000b; Prasad and Enzel, 2006; Breitenbach, 2012; Lupker et al., 2013). For the present data set, we analyzed sediments that span ages from early Holocene to recent (Fig. 2B), yet a plot of $[Sr]_{sil}$ values versus depth, as a proxy for age, shows no systematic trends or variation (Fig. S3A [see footnote 1]). This suggests that any effects of differential weathering in response to climate, or related environmental impacts, are secondary to the differences imparted by initial source-rock geochemistry. Thus, $[Sr]_{sil}$ appears to remain a useful proxy for sediment provenance over millennial time scales, at least through the Holocene. To note, though, Lupker et al. (2013) demonstrated that the degree of weathering for Ganges-Brahmaputra sediments reaching the Bengal shelf and fan has increased since the Last Glacial Maximum. This enhanced sediment weathering is reflected in their observation of declining K/Si ratios and calcite abundance toward present. Therefore, to confirm our observation of limited changes in weathering for the present data set, we plotted K_2O/SiO_2 versus depth (Fig. S3B [see footnote 1]). Results show no significant trend, or perhaps a slight increase in younger sediments. The latter may represent either a slight decrease in weathering or be a consequence of the overall upward fining of sediment grain size (Goodbred and Kuehl, 2000a).

Although it has been established that Sr within Bengal basin sediments is primarily associated with plagioclase, the possible effects of biotite weathering on $^{87}Sr/^{86}Sr$ ratios should also be considered. Micaceous minerals are often concentrated in finer grain-size classes and may yield exceedingly high $^{87}Sr/^{86}Sr$ values >0.900 (Blum and Erel, 1997). Sediments in the Ganges-Brahmaputra-Meghna delta have been recognized to contain up to 30% mica in sandy samples and up to 80% in silty deposits (Huizing, 1971; Derry and France-Lanord, 1996). To test this potential complication, we plotted MgO versus Al_2O_3/SiO_2, which shows a modest depletion of Mg and suggests some preferential weathering of biotite in finer size classes (Fig. S3C [see footnote 1]). However, a plot of $^{87}Sr/^{86}Sr$ versus Al_2O_3/SiO_2 shows no trend of Sr isotopes with grain size, indicating that any effect of biotite weathering on Sr isotope values is considerably less than the source signal (Fig. S3D [see footnote 1]).

Hydraulic Sorting

The majority of Sr within detrital sediments of the Bengal basin is constrained to only a few minerals, making Sr concentrations potentially vulnerable to hydraulic sorting. From the bulk-sediment geochemistry of modern Ganges and Brahmaputra bed load, Garzanti et al. (2010) calculated that Ca-plagioclase and lithic fragments contribute ~80% of Sr for typical Ganges sediment and ~75% for the Brahmaputra. Of the remaining Sr fraction, 10%–20% may be contributed by the heavy minerals epidote (3.4 g/cm^3) and amphibole (3.1 g/cm^3). In this case, the dominant association of Sr with plagioclase and lithics should serve to mitigate the effects of hydraulic sorting, because the densities of Ca-plagioclase (2.7 g/cm^3) and lithics (<2.9 g/cm^3) are comparable to those of quartz and coarser clays (2.6–2.8 g/cm^3) that dominate the fluvial sediment load. Toward the tails of the sorting distribution, increased concentrations of heavy minerals and micas within Ganges-Brahmaputra-Meghna delta fluvial deposits do occur at the bed scale (<10 cm). In this study, though, the drilling process by which samples were collected typically integrates sediment over 0.5–1.5 m of stratigraphy, which should largely exclude bias from bed-scale placers formed by hydraulic sorting. Indeed, the only sample to show significant effects of hydraulic sorting in the present data set is the fine (<63 µm) fraction at 84 m depth in Ajmiriganj (Fig. 2). This sample is enriched 3–10-fold in TiO, Cr, Zr, Y, and Nb; however, both $[Sr]_{sil}$ and $^{87}Sr/^{86}Sr$ values for this sample are the same as those for adjacent, nonplacer deposits (Table S1 [see footnote 1]). These findings suggest

that sorting, like weathering, is not a first-order control on the observed patterns in Sr geochemistry for this data set.

Strontium Distribution in Delta Sediments

Results from the bulk geochemical analysis of these sediments indicate that Sr concentrations in the silicate fraction are: (1) modally distributed; (2) not principally a function of grain size or silica content; and (3) not strongly impacted by weathering or hydraulic sorting. Thus, Sr variations may be considered a potentially valid provenance indicator that can be used to distinguish sediments derived from the primary river systems delivering sediment to the Bengal basin. Within the Bengal basin itself, variance in $[Sr]_{sil}$ measures (n = 185) defines a multimodal normal distribution (Fig. 4). The low-Sr and high-Sr groups are each unimodal, with distinct peaks at 91 ppm and 164 ppm, respectively. The mid-Sr group is bimodal, with peaks at 113 and 125 ppm. For the low-Sr group, the range of values is largely coincident with that for the Ganges River catchment (Fig. 4A), where sediments are principally eroded from the High Himalayan Crystalline series, with secondary contributions from the Lesser Himalaya and Indian craton (Singh et al., 2008). The median of published $[Sr]_{sil}$ values for the main-stem Ganges is 75 ppm (Singh et al., 2008), which is generally comparable to the median of 84 ppm for the low-Sr samples from the Bengal basin (Fig. 4C). The two data sets are not equivalent, however, and lower $[Sr]_{sil}$ values for the upstream data set (Singh et al., 2008) likely result from the higher proportion of samples collected in weathered floodplain environments, as compared with the coarser, more rapidly buried Ganges-Brahmaputra-Meghna delta stratigraphy (Fig. 4A; e.g., Lupker et al., 2012). For comparison with a smaller (n = 6) but more equivalent data set, Holocene borehole samples collected along the Ganges at Kanpur, India, have a mean $[Sr]_{sil}$ value of 82 ppm (median of 83 ppm), which is nearly identical with the low-Sr samples from this study (Fig. 4C).

For the group of high-Sr samples, the distribution of $[Sr]_{sil}$ values is coincident with that observed for the main-stem Brahmaputra and is clearly defined by a normal distribution with a prominent mode at 164 ppm (Figs. 4B–4C; Singh and France-Lanord, 2002). However, samples from the Ganges-Brahmaputra-Meghna delta clearly lack the highest ~10% of $[Sr]_{sil}$ values (i.e., >200 ppm) that have been measured along the Assam Valley of the Brahmaputra (Fig. 4B), possibly reflecting dilution with low-Sr Himalayan or Shillong sediments (e.g., Singh et al., 2008). It should be noted that the main-stem Brahmaputra values are entirely discrete from the $[Sr]_{sil}$ values of its tributaries in Assam, which are sourced from High Himalayan Crystalline rocks to the north and the Shillong Massif to the south (Fig. 1). The reason for such distinct values between the main-stem Brahmaputra and its Assam tributaries is that the latter contribute relatively little sediment compared with upstream sources originating around the eastern Himalayan syntaxis (Fig. 1). The syntaxis is among the most rapidly eroding regions on Earth, draining large exposures of the Trans-Himalayan batholiths, which are comparatively high in $[Sr]_{sil}$ (Singh and France-Lanord, 2002; Garzanti et al., 2004; Stewart et al., 2008).

The Ganges-Brahmaputra-Meghna delta data set also has a significant proportion (28%) of samples having intermediate $[Sr]_{sil}$ values, ranging 100–140 ppm, with modes at 113 ppm and 125 ppm (Fig. 4C). The 113 ppm peak corresponds with a similar mode in the Ganges catchment data, although these samples overlap with neither the main-stem Ganges nor Brahmaputra values. Thus, the origin of these sediments remains indeterminate based on Sr concentrations alone but can be better evaluated with consideration of their Sr and Nd isotope signatures.

Strontium and Neodymium Isotopes

The $^{87}Sr/^{86}Sr$ results show that Holocene Ganges-Brahmaputra-Meghna delta sediments fall within the modern range of 0.720–0.781 measured for the main-stem rivers (Fig. 5A). More specifically, $^{87}Sr/^{86}Sr$ values plotted with Sr concentrations reveal that most results from the Bengal basin fall along mixing curves defined by the Ganges and Brahmaputra end members, with relatively lower $[Sr]_{sil}$ and higher $^{87}Sr/^{86}Sr$ for the Ganges-derived sediments compared with higher $[Sr]_{sil}$ and lower $^{87}Sr/^{86}Sr$ for Brahmaputra-derived sediments (Fig. 5A). A third field of data has both low $[Sr]_{sil}$ and low $^{87}Sr/^{86}Sr$ values and is similar to those measured for streams draining the Shillong Massif, although available data are limited for this region (n = 6) and show high variability (Fig. 5A; Singh and France-Lanord, 2002). Another likely source of sediment with low $^{87}Sr/^{86}Sr$ and low $[Sr]_{sil}$ is the Neogene deltaic sections of the Tripura fold belt (Figs. 1 and 2), which were originally sourced from the Brahmaputra-Himalayan dispersal system before being uplifted (Allen et al., 2008). Sediments eroding from this region now represent second-generation recycled material with attendant loss of weatherable minerals, such as the Sr-bearing plagioclase feldspars.

The distribution of these low $^{87}Sr/^{86}Sr$, low $[Sr]_{sil}$ sediments is geographically restricted to the central and eastern portions of the Sylhet basin (Fig. 2; sites 15, 16). This area is fed directly by the Surma River (cf. Barak River in India), which drains portions of the eastern Shillong Massif and a large area of the Tripura fold belt (Fig. 1). As the only large river entering the eastern Sylhet basin, the Surma River is almost certainly the fluvial source for the low $^{87}Sr/^{86}Sr$, low $[Sr]_{sil}$ sediments recovered in this area. Research is currently under way to identify specific contributions from the Surma River sediment load, but given current uncertainty, we henceforth refer to these low $^{87}Sr/^{86}Sr$, low $[Sr]_{sil}$ sediments as being Sylhet-sourced, implicitly including both Shillong- and Tripura-derived inputs.

The vast majority of Sr results from this study fall along mixing curves between the Ganges, Brahmaputra, and Sylhet end members, indicating that these are the three principal sources of Holocene sediment delivered to the Bengal basin and constructing the Ganges-Brahmaputra-Meghna delta (Fig. 5A). However, for a more direct comparison with previous isotope studies, a subset of samples was also analyzed for Nd isotopes. These results, plotted with the $^{87}Sr/^{86}Sr$ data, reflect the well-recognized distinction between Ganges and Brahmaputra fluvial sediments (Fig. 5B; e.g., Derry and France-Lanord, 1996; Galy and France-Lanord, 2001; Singh and France-Lanord, 2002). These distinctions follow the more negative ε_{Nd} values of Ganges sediment that are imparted by the High Himalayan Crystalline Sequence and Lesser Himalaya source rocks, as compared with the higher ε_{Nd} values contributed by the Brahmaputra's Trans-Himalayan batholith sources (Fig. 5B). Existing data for tributaries draining the Shillong Massif, however, show considerable variation, and their mean $^{87}Sr/^{86}Sr$ and ε_{Nd} values are largely indistinguishable from those of the Brahmaputra (Fig. 5B). In this case, it is the application of $[Sr]_{sil}$ versus ε_{Nd} that proves useful in distinguishing Sylhet-derived sediments from those of the Brahmaputra, underscoring the importance of Sr concentrations for provenance analysis in the region (Fig. 5C).

DISCUSSION

One of the principal results to emerge from the aggregate data set of Ganges-Brahmaputra-Meghna delta sediments is that all observations fall squarely within the ranges defined by modern fluvial sediment (Figs. 5 and 6), suggesting that there has been no major change in their Sr signatures through the Holocene. The range of Sr and Nd geochemical data further indicates that sediments infilling the Bengal basin over the last 10,000 yr have been primarily derived from the Ganges and Brahmaputra Rivers, with

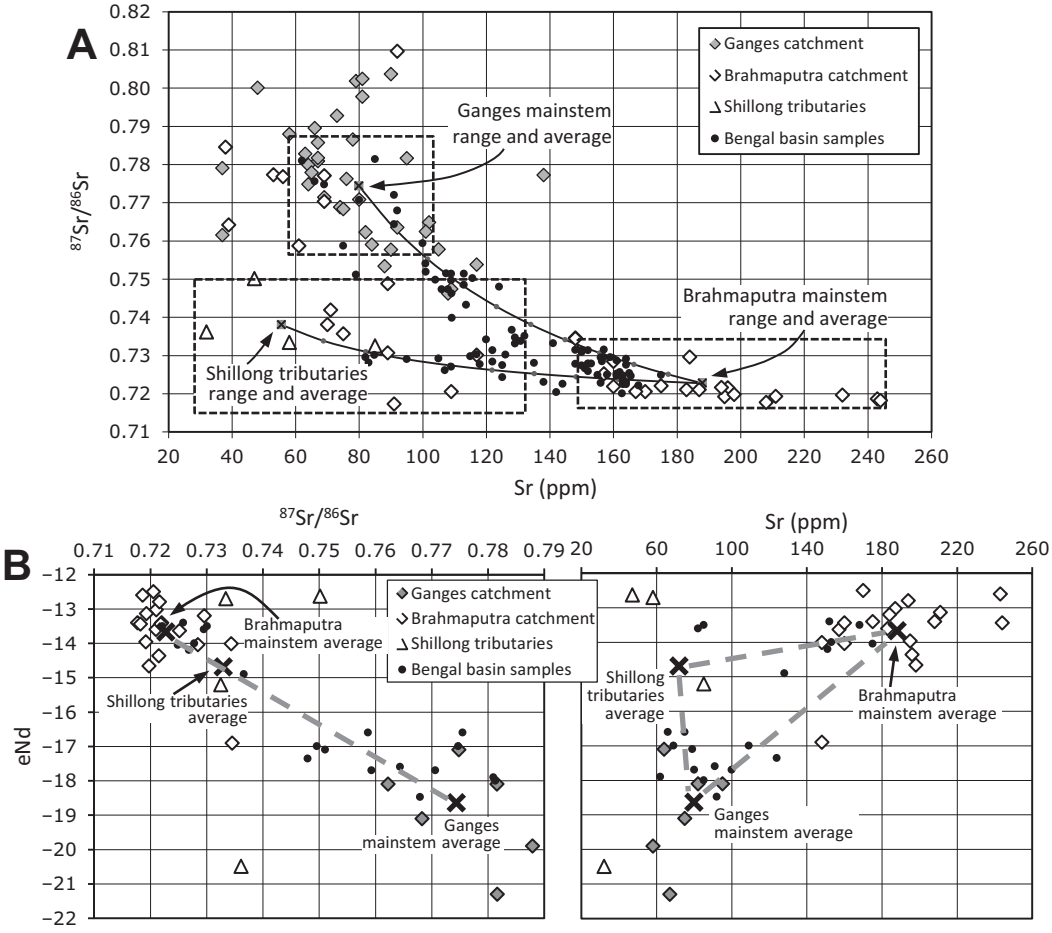

Figure 5. Comparison of $[Sr]_{sil}$ with Sr and Nd isotopes for silicate sediments from the main river catchments and the Bengal basin (this study; Singh and France-Lanord, 2002; Singh et al., 2008). (A) Plot of $[Sr]_{sil}$ vs. $^{87}Sr/^{86}Sr$ reveals the distinct geochemical signatures of Brahmaputra-, Ganges-, and Shillong-derived sediments, with Holocene sediments from the Bengal basin plotting well within the range of these three sources. (B) $^{87}Sr/^{86}Sr$ vs. ε_{Nd} for bulk sediments from the source catchments compared with Bengal basin sediments. Previously, Sr and Nd isotopes have been employed for provenance studies, but here the signatures of Shillong- and Brahmaputra-derived sediments are not as distinct as the relationships in A. Groupings are generally more distinct in the plot of $[Sr]_{sil}$ vs. ε_{Nd} (B); however, the $^{87}Sr/^{86}Sr$ vs. $[Sr]_{sil}$ plot is most beneficial in tracing provenance of Bengal basin sediments.

locally significant inputs from streams draining the Shillong Massif and Tripura fold belt. However, many deposits also comprise intermediate compositions that lie along mixing curves between these three end members (Fig. 7). Such intermixing of different sediment sources may preferentially occur (1) below river channel confluences, (2) through mixing in the coastal zone, or (3) through postdepositional reworking during channel migration or avulsion.

Distribution of Fluvial Sediment Sources in the Bengal Basin

Following historical observations and evidence from the stratigraphic record, rivers of the region are known to exhibit avulsive, migratory channel behavior (Fergusson, 1863; Addams-Williams, 1919; Morgan and McIntire, 1959; Goodbred and Kuehl, 2000a; Best et al., 2007). Thus, when placed in a spatial framework, the distribution of high-Sr, low-Sr, and intermediate-Sr samples reveals clear, first-order patterns within Bengal basin stratigraphy (Fig. 6). This application of provenance tracers presents a major step toward unraveling the timing and location of the major river channels in response to endogenous, or autocyclic, behaviors, as well as their exogenous forcing through variation in climate, sea-level rise, and tectonic deformation.

Stratigraphy in the western portions of the Ganges-Brahmaputra-Meghna delta consists of almost entirely low-Sr sediments of Ganges origin (Fig. 6; sites 1–4). This dominance of Ganges sediment holds throughout the Holocene stratigraphy, including the 90-m-long core at Jessore (site 1) that was drilled within the river's lowstand valley (Goodbred and Kuehl, 2000a). Evidence for Ganges-sourced sediment is found further east as well, particularly in the shallow, upper Holocene stratigraphy of the central delta (Fig. 6; sites 5–8). However, the Ganges is not the sole sediment source at these locations, with most of the deeper stratigraphy having a mixed or Brahmaputra end-member signal. These findings appear to confirm previous speculation that the Ganges was mostly confined to the western delta during the early–mid-Holocene and did not flow as far east as its current path until the late Holocene (Allison et al., 2003). In contrast, coarse channel sands from the Brahmaputra River are found well west of its current course in the lower to middle Holocene stratigraphy at Narail (site 5; Figs. 2, 6, and 7A), providing the first evidence for the river west of the Jamuna Valley. Much of the stratigraphy at Narail is actually of mixed origin, with some end-member Ganges sediment in the upper Holocene, indicating that the site has hosted both channels and may intermittently serve as a confluence point.

In the eastern portions of the lower delta plain (sites 9–12), Sr signatures indicate that the Brahmaputra River has been the dominant source of sediment throughout the Holocene (Fig. 6). This appears to confirm that the modern course of the Ganges represents only a recent channel configuration that is not likely to have occurred previously in the Holocene. The ubiquitous Brahmaputra signature at sites 9–12 is also consistent with this braided river being a highly mobile system and occupying multiple courses through the Holocene, including its modern course along the Jamuna Valley and its Old Brahmaputra course via the Sylhet basin (Fig. 2; Goodbred and Kuehl, 2000a; Pickering et al., 2013). Within the Sylhet basin itself (sites 13–16), high-Sr values continue to show

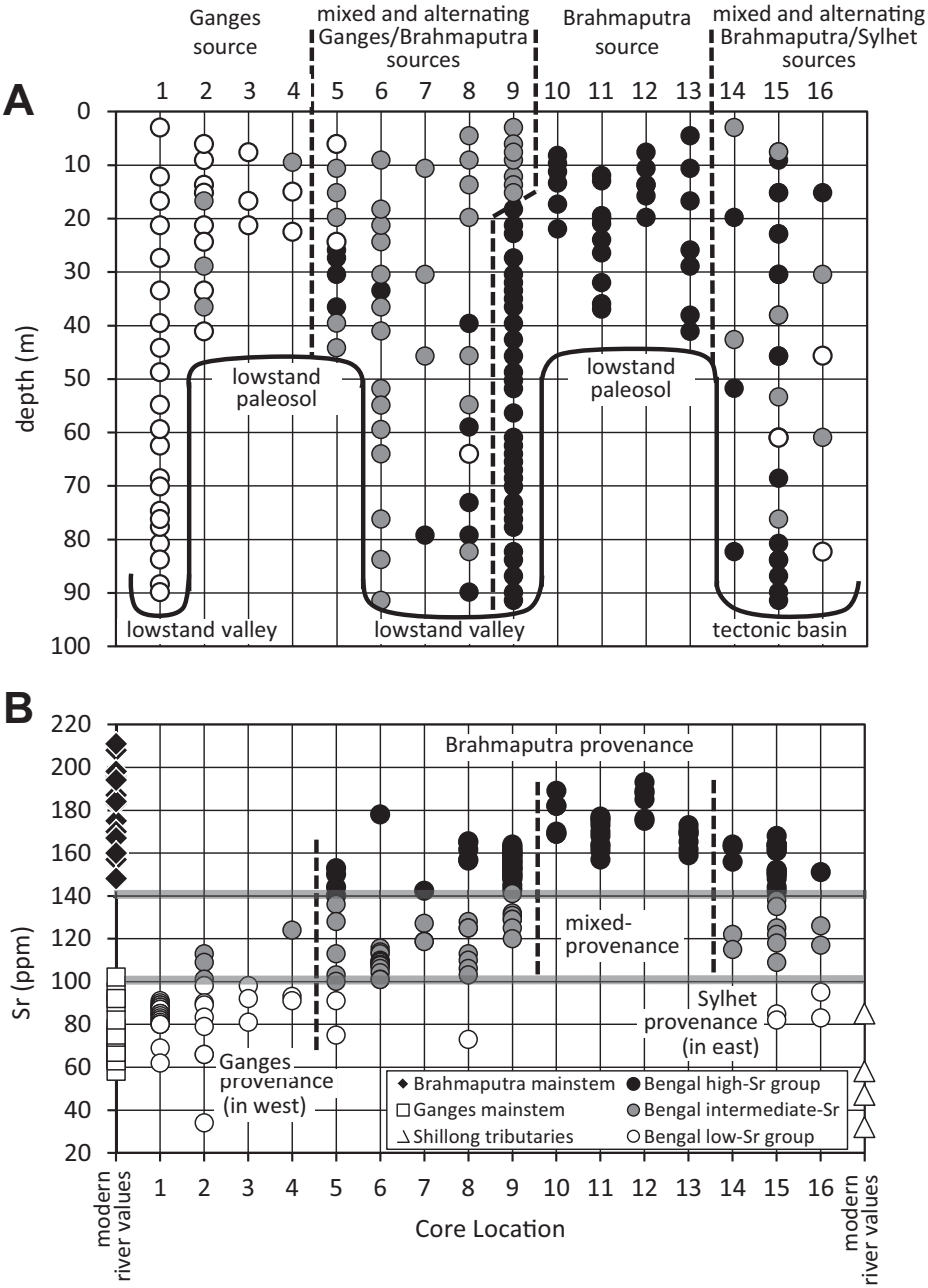

Figure 6. (A) Depth distribution of high-Sr, medium-Sr, and low-Sr groups for each core, and (B) the range of Sr concentration for each core in comparison with values for the modern rivers. In each panel, it can be seen that Ganges-derived sediments are limited primarily to the western Ganges-Brahmaputra-Meghna delta, whereas Brahmaputra sediments dominate the eastern portions. Notable mixing zones occur in the central delta and within Sylhet basin.

a major influence of Brahmaputra sediments throughout the Holocene, particularly along the Old Brahmaputra course (Fig. 2). However, the Sr signatures are not exclusively Brahmaputra, with about one third of the stratigraphy in Sylhet basin having intermediate- to low-Sr values. These lower-Sr values indicate periods when Brahmaputra input was absent from the Sylhet basin, or else diluted by low-Sr sediment from the Surma River. The Surma River is the principal stream draining the eastern Shillong Massif and northern Tripura fold belt, discharging an estimated 36.5×10^6 t/yr of sediment, or ~7% that of the Brahmaputra (Khan et al., 2005).

Interpreting Mixed Lithologies

Stratigraphy in two principal areas of the Bengal basin is dominated by variable source inputs: (1) the central delta plain, with joint Ganges and Brahmaputra influence, and (2) the Sylhet basin, with mixed Brahmaputra-Sylhet inputs (Figs. 6 and 7). At a first order, these areas of mixed input contrast with areas that are characterized only by end-member lithologies, suggesting that river courses are not randomly spaced through time but rather have preferred pathways, perhaps under geomorphic or structural control.

Central delta plain. In the central delta, plots of $[Sr]_{sil}$ versus $^{87}Sr/^{86}Sr$ reveal three largely discrete sediment populations (Fig. 7A). Two of these populations exhibit end-member signatures of the Ganges and Brahmaputra, having generally more radiogenic, low-Sr values versus less radiogenic, high-Sr sediments, respectively. Along the mixing curves lies a third data cluster with a distinctly intermediate-Sr composition (Fig. 7A). Within this group, most samples are from a single borehole in the south-central delta plain (Bagerhat, site 6); yet samples having the same or similar Sr signatures are also recognized in three other boreholes to the north and west (sites 2, 5, and 8; Fig. 7A). At face value, the Sr signatures of this group indicate an intermediate composition that corresponds to a mixing ratio of roughly 3:2 of sediments from the Ganges and Brahmaputra Rivers. A comparison of the results from Bagerhat with other sites (site 6; Figs. 2 and 8A–8B) also shows that the Sr geochemistry is entirely nonoverlapping with nearby cores, which are dominated by either Ganges or Brahmaputra end-member inputs (sites 1 and 9, respectively). For perspective, these discretely intermediate-Sr signatures persist through major changes in lithology (sands to muds) and encompass 90 m of Holocene stratigraphy deposited over 10,000 yr (Fig. 2B). This exclusive separation of geochemical signatures within the Holocene central delta plain again suggests that the Ganges-Brahmaputra-Meghna delta fluvial channel network is nonrandomly distributed and likely exhibits preferred patterns of organization over millennial time scales.

These results suggest that the Ganges and Brahmaputra Rivers have jointly occupied the Bagerhat area (site 6) several times in the Holocene, depositing a heterogeneous stratigraphy with a reasonably stable ratio of sediment input between the two systems. Although conceivable, this is not a trivial outcome given the different discharge of these rivers, the different mud:sand ratios of their sediment loads, their migratory and avulsive behavior, and considerable changes in climate and eustasy through the Holocene (Fergusson, 1863; Addams-Williams,

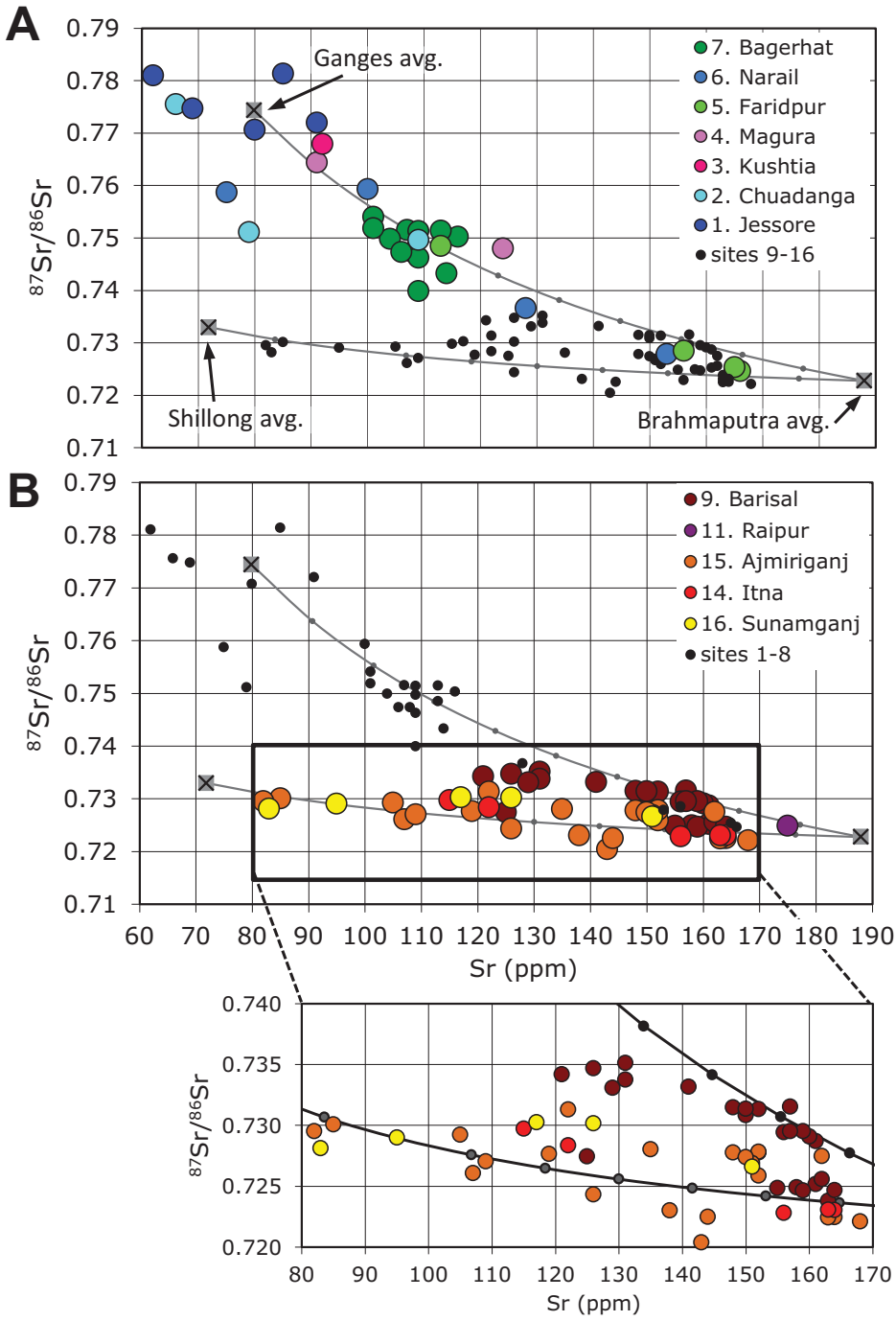

Figure 7. Plots of $[Sr]_{sil}$ vs. $^{87}Sr/^{86}Sr$ for the Bengal basin data set, including mixing curves calculated from average end-member values for the Ganges-, Brahmaputra-, and Shillong-sourced sediments (Singh and France-Lanord, 2002; Singh et al., 2008). Data presented in color on the upper panel (A) correspond to core locations from the west-central delta (Fig. 2; sites 1–8), and cores from the eastern delta (Fig. 2; sites 9–16) are highlighted in the lower panel (B). In panel A, three distinct populations are evident along the Ganges-Brahmaputra mixing curve, identifying those sediments that are either Ganges or Brahmaputra in origin, with a third population of intermediate composition recovered primarily at site 6 but also sites 2, 4, and 8. These intermediate-composition sediments suggest a 3:2 mixing ratio of Ganges and Brahmaputra sediment. In panel B, results from the eastern portion of the delta reveal Brahmaputra-dominated sediments that are locally mixed with sediment from the Sylhet basin rivers sourced from the Shillong Massif and Tripura fold belt (Figs. 1 and 2). The panel B inset highlights fine structure in the data showing Brahmaputra sediments to track one or the other mixing curve, presumably a consequence of incorporating minor amounts of Ganges- or Sylhet-derived sediment when the river is flowing along its western Jamuna course or eastern Sylhet course, respectively.

Figure 8 (*on following page*). Plots of $^{87}Sr/^{86}Sr$ and [Sr] vs. depth reflecting shifts in fluvial sediment inputs for three regions in the delta. Note that values for $^{87}Sr/^{86}Sr$ have been reversed on the *x*-axis so that data trends are oriented as they are for Sr concentrations. (A, B) Results from the lowstand valleys of the Ganges (site 1: Jessore), Brahmaputra (site 9: Barisal), and a site of intermediate composition (site 6: Bagerhat) show discrete Sr signatures that suggest the relative stability of these source signals throughout the Holocene. (C, D) Results from the central delta plain capture the geochemical record of the Ganges' eastward migration during the mid-late Holocene, with perhaps some earlier distributary connections suggested in the [Sr] results. (E, F) In the Sylhet basin, Sr signatures record several shifts (avulsions) of the Brahmaputra between its Jamuna and Old Brahmaputra courses, as well as the mixing of Brahmaputra sediments with locally derived sediments from the Sylhet region.

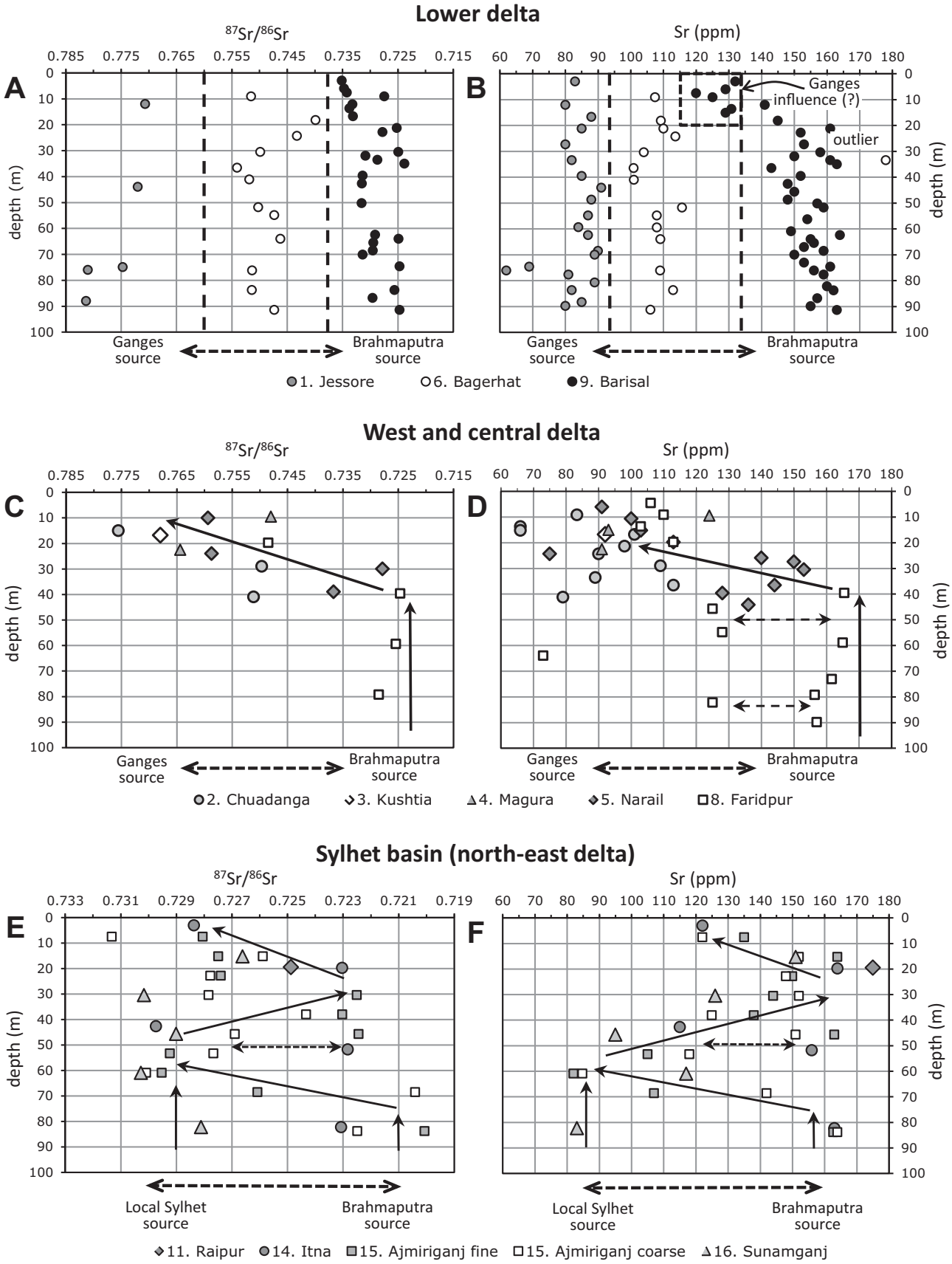
Lower delta
87Sr/86Sr
Sr (ppm)
A
B
depth (m)
Ganges influence (?)
outlier
Ganges source
Brahmaputra source
1. Jessore
6. Bagerhat
9. Barisal
West and central delta
C
D
2. Chuadanga
3. Kushtia
4. Magura
5. Narail
8. Faridpur
Sylhet basin (north-east delta)
E
F
Local Sylhet source
11. Raipur
14. Itna
15. Ajmiriganj fine
15. Ajmiriganj coarse
16. Sunamganj

Figure 8.

1919; Morgan and McIntire, 1959; Coleman, 1969; Goodbred and Kuehl, 2000a; Best et al., 2007). One plausible mechanism for the persistent intermediate-Sr signatures at Bagerhat may be the mixing of different sediment loads by tides and other coastal processes. The presence of mangrove wood and brackish gastropods (*Littorina* sp.) in Bagerhat stratigraphy indicate that the site was an estuarine environment for at least part of the Holocene (Goodbred and Kuehl, 2000a). In this case, strong, bidirectional tidal currents have been active along the Bengal margin throughout the Holocene and should provide an effective and persistent mechanism for sediment mixing and the generation of intermediate geochemical signatures at Bagerhat. Indeed, the mean $^{87}Sr/^{86}Sr$ value of 0.749 ± 0.004 for Bagerhat sediments is comparable to the mean of 0.744 ± 0.005 for Holocene-age sediments collected from the presumably well-mixed sediments of the Bengal shelf and deep-sea fan systems (Lupker et al., 2013).

Sylhet basin mixing zone. For sediments of the Sylhet basin (sites 14–16), plots of Sr geochemistry show Holocene deposits to lie in a continuum along the Shillong-Brahmaputra mixing curve (Fig. 7B). These results also show that sediments in the Sylhet basin yield few end-member Sr values, with nearly all data reflecting a variable mixing of Brahmaputra- and Sylhet-sourced sediments. The only deposits that do have a clear end-member signature are those of Brahmaputra channel sands recovered at Itna in the western basin (site 14; Figs. 2 and 7B inset). These results are consistent with previous evidence that places the Brahmaputra River along its Old Brahmaputra course several times in the Holocene (Goodbred and Kuehl, 2000a; Pickering et al., 2013). However, toward the central and eastern portions of Sylhet basin (sites 15, 16), sediments almost universally yield a mixed Sr signature, indicating that they represent inputs from both Brahmaputra and local Sylhet sources, the latter presumably dominated by Surma River inputs. The sediment lithology of this region is also considerably finer than in most of the Ganges-Brahmaputra-Meghna delta, comprising a thick succession of silt and clay with intermixed fine sand (Fig. 2B). Together, the fine heterolithic stratigraphy and intermediate-Sr values indicate that sedimentation in the Sylhet basin is sustained through overbank and splay deposition from the Brahmaputra River, Surma River, and related local tributaries.

Distinguishing Brahmaputra channel courses. On the east-central delta plain, the Sr geochemistry at Barisal (site 9; Fig. 2) can be seen to define two distinct Brahmaputra-dominated sediment populations, each tracking either the Ganges-to-Brahmaputra mixing curve or the Shillong-to-Brahmaputra curve (Fig. 7B inset). These distinctions appear modest, but the measured differences in Sr isotopes (~0.05–0.10) and Sr concentrations (20–40 ppm) are much greater than the analytical precision (<0.000025 and ± 5 ppm, respectively). Thus, these differences almost certainly reflect real variance in the data. As such, sediments falling along the different mixing curves appear to record switching of the Brahmaputra River between its two courses through the Jamuna Valley and Sylhet basin.

For example, when the Brahmaputra occupies its Jamuna course, sediments appear to acquire a slight Ganges signature that presumably develops as the channel transits the central delta plain, which is also partially influenced by Ganges input (Fig. 2). In contrast, Brahmaputra sediments appear to acquire a slight Sylhet-sourced Sr signature when occupying the Old Brahmaputra course that is proximal to the Surma River, although the magnitude of this effect is less than that for the Ganges-influenced deposits (Fig. 7B inset). This latter finding would be consistent with the comparatively smaller discharge of the Surma River relative to the Brahmaputra (Khan et al., 2005). For sediments at Barisal, they fall predominantly along the Ganges mixing curve (Fig. 7B inset), implying that Jamuna Valley has been the preferred course for the Brahmaputra through the Holocene. This finding is entirely consistent with the much greater dimensions of the upstream Jamuna Valley compared with its Old Brahmaputra counterpart (Pickering et al., 2013). These Sr results also indicate that (1) sediments at Barisal may consist of up to ~25% Ganges-derived material and (2) little locally sourced sediment (i.e., Surma River) has escaped the Sylhet basin during the Holocene.

Fluvial Channel Histories and Delta Evolution

Placing these observations into a spatiotemporal framework, it is possible to reconstruct some of the major fluvial channel movements that have occurred during the Holocene (Fig. 8; Heroy et al., 2003). Among all cores, three sites yield thick (>90 m), uniformly sandy stratigraphy with no lowstand paleosol surface, indicating that these boreholes were drilled within lowstand valleys (Figs. 2B and 8A; Goodbred and Kuehl, 2000a; Sarkar et al., 2009). The end-member Sr signatures measured at Jessore and Barisal demonstrate that these sites occupy the Ganges and Brahmaputra lowstand valleys, respectively (Figs. 8A–8B). Furthermore, the Sr signatures at these sites have remained remarkably stable through the Holocene, suggesting that these valleys represent preferred channel pathways for the two rivers. The one clear deviation recorded at these sites lies in the shallow (<20 m) stratigraphy at Barisal, where Sr concentrations (Fig. 8B) and Sr isotopes (Figs. 7B [inset] and 8A) indicate modest influence from the Ganges in the late Holocene. These particular sediments are also fine grained and may reflect mixing of suspended load within the late Holocene river-mouth estuary (cf. Allison et al., 2003), which is the same mechanism suggested for the intermediate values recorded at Bagerhat (Figs. 8A–8B).

Brahmaputra Channel Avulsions

Stratigraphy in the northeast delta and Sylhet basin records three main phases of Brahmaputra channel evolution during the Holocene. Evidence for the first postglacial input of Brahmaputra sediment to Sylhet basin is provided by medium to coarse sands at Itna that have an end-member Brahmaputra Sr signature (site 15; Figs. 2B and 8E–8F; Pickering et al., 2013). In the eastern Sylhet basin at this same time, medium to coarse sands deposited at Sunamganj (site 16) have a locally sourced end-member Sr signature, indicating that both rivers contributed to sediment deposition at this time. However, the shift to finer-grained sediments and a locally sourced Sr signature at all Sylhet basin sites suggests that Brahmaputra influence in the early Holocene was relatively brief (Pickering et al., 2013). We note, however, that observed changes in Sr geochemistry are not a function of the shift to finer-grained sediment, which we tested by separating the coarse (fine sand) and fine (clayey silt) fractions and measuring their Sr geochemistry separately (Figs. 8E–8F).

Overall, these results confirm that the Brahmaputra principally occupied its Jamuna Valley course from the early Holocene to at least 7 ka (Fig. 9). During this time, however, the relatively gradual changes in Sr geochemistry observed in Sylhet basin stratigraphy suggest that the avulsion may have occurred gradually, with the Brahmaputra maintaining some connection with Sylhet basin over an extended period (10^2 yr). This behavior would be comparable to the river's historical avulsion into the Jamuna channel, which initiated in the late eighteenth century and has since maintained wet-season discharge through the "abandoned" Old Brahmaputra channel (Fergusson, 1863; Bristow, 1999; Best et al., 2007). Such intermittent distributary connections with the Sylhet basin may also be reflected by the thin lenses of high-Sr sediment that are recorded at ~50 m depth at Itna and Ajmiriganj (sites 14–15; Figs. 8E–8F).

Beginning ca. 7 ka to ca. 5 ka, Sr signatures at 10–40 m depth reveal a major reoccupation of the Sylhet basin by the Brahmaputra River (Figs. 2, 8E–8F, and 9B). This episode of

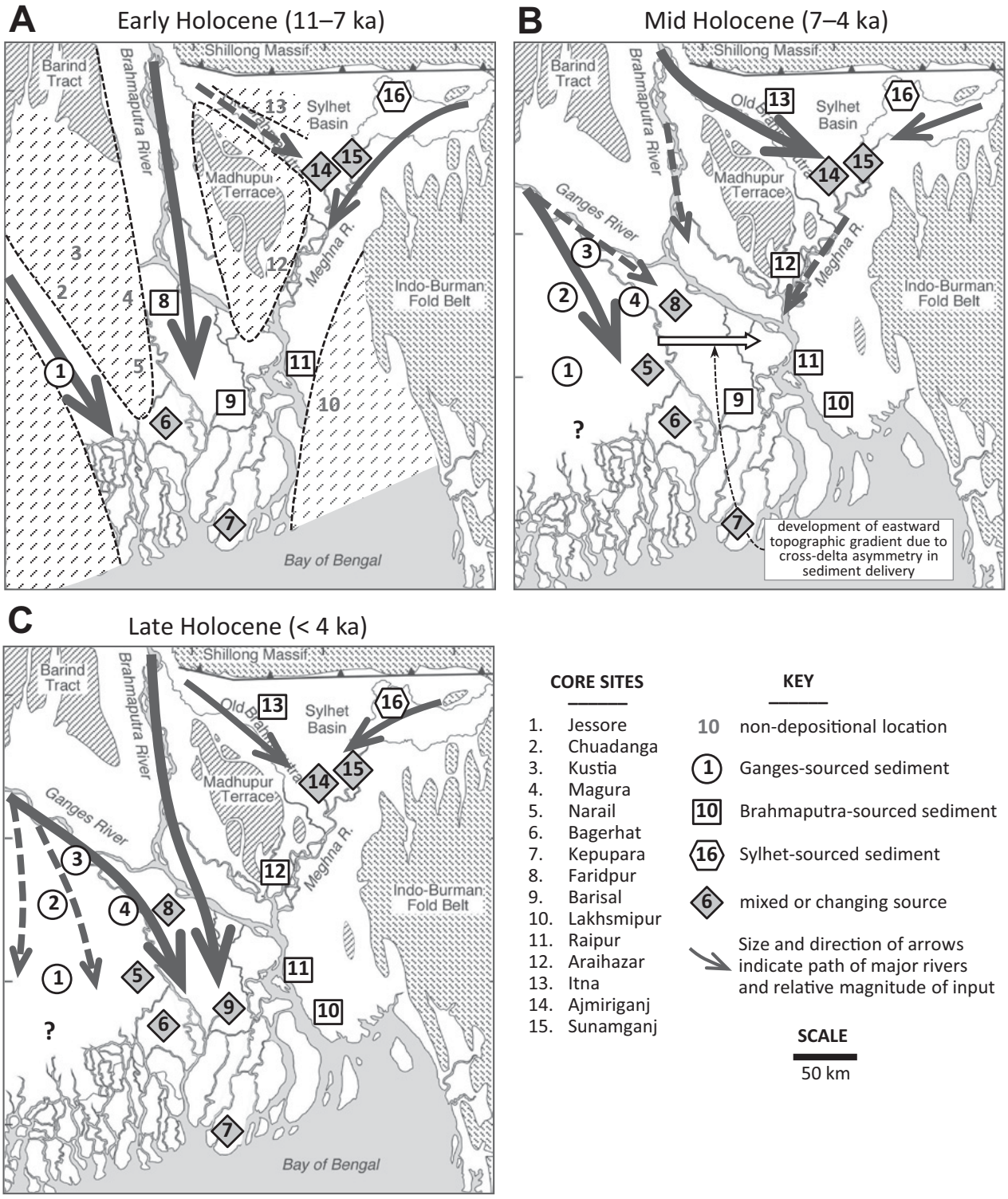

Figure 9. Schematic reconstruction of river pathways and general sediment distribution patterns associated with the Ganges, Brahmaputra, and Sylhet sources through the Holocene. Base map from Figure 1. Patterns are based on geochemical provenance records from this study and are generally consistent with earlier lithology-based interpretations (Umitsu, 1993; Goodbred and Kuehl, 2000a). (A) Rivers during the early Holocene are constrained within their lowstand valleys, with limited Brahmaputra influence in Sylhet basin. (B) Slowed sea-level rise allows rivers to infill accommodation and drives increased mobility across the delta, with Ganges trending east and Brahmaputra occupying Sylhet basin. (C) The main rivers interact on the central delta plain in the late Holocene, shifting toward the modern confluence and shared river-mouth estuary.

significant deposition by the Brahmaputra had been suggested in previous research based on apparently rapid sediment accretion and large inputs of sand (Goodbred and Kuehl, 2000a; Pickering et al., 2013). Here, the clear Brahmaputra signatures from the Sr data set appear to confirm this important period in Ganges-Brahmaputra-Meghna delta history. This routing of the Brahmaputra through the Sylhet basin also corresponds with maximum transgression in the eastern delta, as the coast was starved of sediment due to its upstream sequestration in the subsiding basin (Goodbred and Kuehl, 2000a). Beginning ca. 5 ka, the Brahmaputra abandoned Sylhet basin and reoccupied the Jamuna Valley, which is recorded by lower Sr values in Sylhet basin due to declining Brahmaputra input relative to locally sourced Sylhet sediments (Figs. 8E–8F). However, the intermediate-Sr (i.e., mixed) values of these shallow deposits (<20 m) suggest that the Brahmaputra maintained some connection with the Sylhet throughout the late Holocene. Indeed, the river occupied its Sylhet course at the time of European exploration around the sixteenth century, only avulsing back to its current course in the Jamuna Valley in the early nineteenth century (Fergusson, 1863; Morgan and McIntire, 1959; Coleman, 1969).

Eastward Shifting of the Ganges and Relation to the Brahmaputra

In the west-central delta plain, the stratigraphy at four locations (sites 2, 4, 5, and 8) effectively records the eastward shifting of the Ganges River through the mid- to late Holocene (Figs. 8C–8D). The best evidence of this shift is recorded at Faridpur (site 8), which lies along the axis of the Jamuna Valley just south of the modern confluence (Fig. 2). At this site, Sr isotopes show that the lower stratigraphy (30–90 m) is dominated by an end-member Brahmaputra signature, but there is a shift to mixed, Ganges-influenced values in the upper 30 m of the stratigraphy (Fig. 8C). Strontium concentrations also reflect this eastward migration of the Ganges, but small excursions in the deeper stratigraphy (>40 m) suggest that there may have been pulsed Ganges inputs earlier in the Holocene (Fig. 8D). Historically, the Ganges River is known to have had east-flowing distributaries connecting with the Brahmaputra (Addams-Williams, 1919), and so similar offtakes may explain these smaller Sr excursions without requiring a full avulsion (Figs. 9A–9B). Taken together, these Sr results and their associated radiocarbon ages (Fig. 2) indicate a coherent, but gradual, shift toward increasing Ganges influence in the central and eastern delta from the mid Holocene (ca. 6 ka) to present (Figs. 8 and 9; e.g., Allison et al., 2003). These results imply that Ganges channel behavior is characterized more by migration and gradual distributary shifts than by abrupt avulsion.

Eastward migration of the Ganges also corresponds with the Brahmaputra's final stage of occupation in the Sylhet basin and maximum marine transgression in the eastern delta (Figs. 8C–8D; Goodbred and Kuehl, 2000a; Allison et al., 2003). We suggest that these fluvial-channel and delta-system behaviors are not coincidental and propose that migration of the Ganges at this time was driven by development of an eastward-tilted topographic gradient (Fig. 9B). Such a gradient would have developed in response to the asymmetric input of Ganges sediment to the western delta at the same time that Brahmaputra sediment was being sequestered within the Sylhet basin, leaving the lower, east-central delta sediment starved (Fig. 9B). Such topographic steering is one of the principal mechanisms that drives river-channel avulsion (e.g., Jerolmack and Paola, 2007; Reitz et al., 2010) and should reflect one of the most likely ways that river-channel behavior for the Ganges and Brahmaputra systems would be interconnected.

CONCLUSIONS

A total of ~8500 km^3 of Holocene sediment has accumulated in the Bengal basin, providing a vast stratigraphic record from which to reconstruct the history of sediment input, fluviodeltaic processes, and evolution of the Ganges-Brahmaputra-Meghna delta through the Holocene. Here, we demonstrate that bulk-sediment Sr-geochemistry can serve as an effective tracer for the provenance of Ganges-Brahmaputra-Meghna delta deposits, particularly when using both Sr isotopes and concentrations. Sr concentrations may also be used independently as a first-order source proxy, but only after carefully considering potential complications from differential weathering, hydraulic sorting, and grain-size variations. Such complications are shown not to be a significant factor for this data set, presumably aided by rapid sediment burial and a resulting lack of diagenesis during Holocene aggradation of the delta (Goodbred and Kuehl, 2000a). In addition to the reasonably well-studied sediment of the Ganges and Brahmaputra systems, results here also show that sediment locally sourced by the Meghna-Surma River system can be recognized by its distinctively lower Sr concentrations. Such deposits are found to comprise a significant portion of the Sylhet basin stratigraphy, particularly when the Brahmaputra occupies its Jamuna course. At no time during the Holocene, though, have Meghna-Surma sediments contributed significantly to stratigraphy of the main delta downstream of the Meghna Valley.

In the central Bengal basin, we find uniformly discrete provenance signals at several locations in the early to mid-Holocene, which indicate that the main rivers were constrained to their lowstand valleys and provided little opportunity for mixing between sources. By ca. 6 ka, the Ganges channel system began to shift eastward, likely induced by development of a topographic gradient while Brahmaputra sediment was sequestered to the Sylhet basin. By ca. 3 ka, clear signatures of Ganges sediment input to the central delta plain reflect an increasingly significant influence in areas previously dominated by the Brahmaputra. In sum, the results presented here provide a first step toward developing a more detailed and thoroughly documented understanding of Ganges-Brahmaputra River behavior and Holocene delta development. The emerging patterns and responses are consistent with recent efforts to model the style and frequency of river-channel avulsion on aggrading plains (e.g., Reitz et al., 2010). Finally, findings from this initial application of provenance tools are encouraging and suggest that a full history for the Ganges-Brahmaputra-Meghna delta and Bengal basin can be reconstructed with continued efforts.

ACKNOWLEDGMENTS

This research was supported by funding from the National Science Foundation (EAR-0309536, EAR-0345777, and OCE-0630595), the American Chemical Society, and Petroleum Research Fund. We wish to thank Associate Editor Tim Lawton, Eduardo Garzanti, and an anonymous reviewer for their thorough critiques, which led to significant improvements in the manuscript.

REFERENCES CITED

Addams-Williams, C., 1919, History of the Rivers in the Gangetic Delta, 1750–1918: Calcutta, Bengal Secretariat Press, 87 p.

Allen, R., Najman, Y., Cater, A., Barfod, D., Bickle, M., Chapman, H., Garzanti, E., Ando, S., Vezzoli, G., and Parrish, R., 2008, Provenance of the Tertiary sedimentary rocks of the Indo-Burman Ranges, Burma (Myanmar): Burman arc or Himalayan-derived?: Journal of the Geological Society of London, v. 165, p. 1045–1057, doi:10.1144/0016-76492007-143.

Allison, M.A., Khan, S.R., Goodbred, S.L., Jr., and Kuehl, S.A., 2003, Stratigraphic evolution of the late Holocene Ganges-Brahmaputra lower delta plain: Sedimentary Geology, v. 155, p. 317–342, doi:10.1016/S0037-0738(02)00185-9.

Andermann, C., Crave, A., Gloaguen, R., Davy, P., and Bonnet, S., 2012, Connecting source and transport: Suspended sediments in the Nepal Himalayas: Earth and Planetary Science Letters, v. 351–352, p. 158–170, doi:10.1016/j.epsl.2012.06.059.

Aziz, Z., van Geen, A., Stute, M., Versteeg, R., Horneman, A., Zheng, Y., Goodbred, S., Steckler, M., Weinman, B., Gavrieli, I., Hoque, M.A., Shamsudduha, M., and Ahmed, K.M., 2008, Impact of local recharge on arsenic concentrations in shallow aquifers inferred from the electromagnetic conductivity of soils in Araihazar, Bangladesh: Water Resources Research, v. 44, no. 7, W07416, doi:10.1029/2007WR006000.

Best, J.L., Ashworth, P.J., Sarker, M.H., and Roden, J.E., 2007, The Brahmaputra-Jamuna River, Bangladesh, *in* Gupta, A., ed., Large Rivers: Geomorphology and Management: New York, John Wiley & Sons, Ltd., p. 395–433.

Blöthe, J.H., and Korup, O., 2013, Millennial lag times in the Himalayan sediment routing system: Earth and Planetary Science Letters, v. 382, p. 38–46, doi:10.1016/j.epsl.2013.08.044.

Blum, J.D., and Erel, Y., 1997, Rb-Sr isotope systematics of a granitic soil chronosequence: The importance of biotite weathering: Geochimica et Cosmochimica Acta, v. 61, p. 3193–3204, doi:10.1016/S0016-7037(97)00148-8.

Brammer, H., 2014, Bangladesh's dynamic coastal regions and sea-level rise: Climate Risk Management, v. 1, p. 51–62, doi:10.1016/j.crm.2013.10.001.

Breitenbach, S., 2012, Changes in Monsoonal Precipitation and Atmospheric Circulation during the Holocene Reconstructed from Stalagmites from Northeastern India [Ph.D. dissertation]: Potsdam, Germany, Deutsches GeoForschungsZentrum (GFZ) Scientific Technical Report STR 10/06, 191 p., doi:10.2312/GFZ.b103-10060.

Bristow, C.S., 1999, Gradual avulsion, river metamorphosis and reworking by underfit streams: A modern example from the Brahmaputra River in Bangladesh and possible ancient example in Spanish Pyrenees, *in* Smith, N., and Rogers, J., eds., Fluvial Sedimentology VI: International Association of Sedimentologists Special Publication 28, p. 221–230.

Coleman, J.M., 1969, Brahmaputra River: Channel processes and sedimentation: Sedimentary Geology, v. 3, p. 129–239, doi:10.1016/0037-0738(69)90010-4.

Curray, J.R., and Moore, D.G., 1971, Growth of the Bengal deep-sea fan and denudation in the Himalayas: Geological Society of America Bulletin, v. 82, p. 563–572, doi:10.1130/0016-7606(1971)82[563:GOTBDF]2.0.CO;2.

Debon, F., Le Fort, P., Sheppard, S.M.F., and Sonet, J., 1986, The four plutonic belts of the Transhimalaya-Himalaya: A chemical, mineralogical, isotopic, and chronological synthesis along a Tibet-Nepal section: Journal of Petrology, v. 27, p. 219–250, doi:10.1093/petrology/27.1.219.

Derry, L.A., and France-Lanord, C., 1996, Neogene Himalayan weathering history and river $^{87}Sr/^{86}Sr$: Impact on the marine Sr record: Earth and Planetary Science Letters, v. 142, p. 59–74, doi:10.1016/0012-821X(96)00091-X.

Faure, G., and Powell, J.L., 1972, Strontium Isotope Geology: New York, Springer-Verlag, 197 p.

Fedo, C.M., Nesbitt, H.W., and Young, G.M., 1995, Unraveling the effects of potassium metasomatism in sedimentary rocks and paleosols, with implications for paleoweathering conditions and provenance: Geology, v. 23, p. 921–924, doi:10.1130/0091-7613(1995)023<0921:UTEOPM>2.3.CO;2.

Fergusson, J., 1863, On recent changes in the delta of the Ganges: Quarterly Journal of the Geological Society of London, v. 19, p. 321–354, doi:10.1144/GSL.JGS.1863.019.01-02.35.

Finnegan, N.J., Hallet, B., Montgomery, D.R., Zeitler, P.K., Stone, J.O., Anders, A.M., and Liu Yuping, 2008, Coupling of rock uplift and river incision in the Namche Barwa–Gyala Peri massif, Tibet: Geological Society of America Bulletin, v. 120, p. 142–155, doi:10.1130/B26224.1.

Galy, A., and France-Lanord, C., 2001, Higher erosion rates in the Himalaya: Geochemical constraints on riverine fluxes: Geology, v. 29, p. 23–26, doi:10.1130/0091-7613(2001)029<0023:HERITH>2.0.CO;2.

Galy, A., France-Lanord, C., and Derry, L.A., 1996, The late Oligocene–early Miocene Himalayan belt constraints deduced from isotopic compositions of early Miocene turbidites in the Bengal fan: Tectonophysics, v. 260, p. 109–118, doi:10.1016/0040-1951(96)00079-0.

Galy, V., France-Lanord, C., and Lartiges, B., 2008, Loading and fate of particulate organic carbon from the Himalaya to the Ganga-Brahmaputra delta: Geochimica et Cosmochimica Acta, v. 72, p. 1767–1787, doi:10.1016/j.gca.2008.01.027.

Galy, V., France-Lanord, C., Peucker-Ehrenbrink, B., and Huyghe, P., 2010, Sr-Nd-Os evidence for a stable erosion regime in the Himalaya during the past 12 Myr: Earth and Planetary Science Letters, v. 290, p. 474–480, doi:10.1016/j.epsl.2010.01.004.

Garzanti, E., Vezzoli, G., Andò, S., France-Lanord, C., Singh, S.K., and Foster, G., 2004, Sand petrology and focused erosion in collision orogens: The Brahmaputra case: Earth and Planetary Science Letters, v. 220, p. 157–174, doi:10.1016/S0012-821X(04)00035-4.

Garzanti, E., Andò, S., France-Lanord, C., Vezzoli, G., Censi, P., Galy, V., and Najman, Y., 2010, Mineralogical and chemical variability of fluvial sediments: 1. Bedload sand (Ganga-Brahmaputra, Bangladesh): Earth and Planetary Science Letters, v. 299, p. 368–381, doi:10.1016/j.epsl.2010.09.017.

Garzanti, E., Andò, S., France-Lanord, C., Censi, P., Vignola, P., Galy, V., and Lupker, M., 2011, Mineralogical and chemical variability of fluvial sediments: 2. Suspended-load silt (Ganga-Brahmaputra, Bangladesh): Earth and Planetary Science Letters, v. 302, p. 107–120, doi:10.1016/j.epsl.2010.11.043.

Goodbred, S.L., 2003, Response of the Ganges dispersal system to climate change: A source-to-sink view since the last interstade: Sedimentary Geology, v. 162, p. 83–104, doi:10.1016/S0037-0738(03)00217-3.

Goodbred, S.L., and Kuehl, S.A., 1999, Holocene and modern sediment budgets for the Ganges-Brahmaputra River system: Evidence for highstand dispersal of flood-plain, shelf, and deep-sea depocenters: Geology, v. 27, p. 559–562, doi:10.1130/0091-7613(1999)027<0559:HAMSBF>2.3.CO;2.

Goodbred, S.L., and Kuehl, S.A., 2000a, The significance of large sediment supply, active tectonism, and eustasy on margin sequence development: Late Quaternary stratigraphy and evolution of the Ganges-Brahmaputra delta: Sedimentary Geology, v. 133, p. 227–248, doi:10.1016/S0037-0738(00)00041-5.

Goodbred, S.L., and Kuehl, S.A., 2000b, Enormous Ganges-Brahmaputra sediment discharge during strengthened early Holocene monsoon: Geology, v. 28, p. 1083–1086, doi:10.1130/0091-7613(2000)28<1083:EGSDDS>2.0.CO;2.

Goodbred, S.L., Kuehl, S.A., Steckler, M., and Sarker, M.H., 2003, Controls on facies distribution and stratigraphic preservation in the Ganges-Brahmaputra delta sequence: Sedimentary Geology, v. 155, p. 301–316, doi:10.1016/S0037-0738(02)00184-7.

Hanebuth, T.J.J., Kudrass, H.R., Linstädter, J., Islam, B., and Zander, A.M., 2013, Rapid coastal subsidence in the central Ganges-Brahmaputra delta, Bangladesh, since the 17th century deduced from submerged salt-producing kilns: Geology, v. 41, p. 987–990, doi:10.1130/G34646.1.

Heroy, D.C., Kuehl, S.A., and Goodbred, S.L., 2003, Sand- and clay-size mineralogy of the Ganges and Brahmaputra Rivers: Records of river switching and late Quaternary climate change: Sedimentary Geology, v. 155, p. 343–359, doi:10.1016/S0037-0738(02)00186-0.

Huizing, H.G.J., 1971, A reconnaissance study of the mineralogy of sand fractions from East Pakistan sediments and soils: Geoderma, v. 6, p. 109–133, doi:10.1016/0016-7061(71)90029-2.

Jerolmack, D.J., and Paola, C., 2007, Complexity in a cellular model of river avulsion: Geomorphology, v. 91, p. 259–270, doi:10.1016/j.geomorph.2007.04.022.

Khan, A.S., Masud, M.S., and Palash, W., 2005, Hydrological Impact Study of Tipaimukh Dam Project of India on Bangladesh: Dhaka, Bangladesh, Institute for Water Modeling, 88 p.

Kuehl, S.A., Allison, M.A., Goodbred, S.L., and Kudrass, H.-R., 2005, The Ganges-Brahmaputra delta, *in* Giosan, L., and Bhattacharya, J., eds., Deltas—Old and New: Society for Sedimentary Geology (SEPM) Special Publication 83, p. 413–434.

Lupker, M., France-Lanord, C., Lavé, J., Bouchez, J., Galy, V., Métivier, F., Gaillardet, J., Lartiges, B., and Mugnier, J.-L., 2011, A Rouse-based method to integrate the chemical composition of river sediments: Application to the Ganga basin: Journal of Geophysical Research, v. 116, F04012, doi:10.1029/2010JF001947.

Lupker, M., France-Lanord, C., Galy, V., Lavé, J., Gaillardet, J., Gajurel, A.P., Guilmette, C., Rahman, M., Singh, S.K., and Sinha, R., 2012, Predominant floodplain over mountain weathering of Himalayan sediments (Ganga basin): Geochimica et Cosmochimica Acta, v. 84, p. 410–432, doi:10.1016/j.gca.2012.02.001.

Lupker, M., France-Lanord, C., Galy, V., Lavé, J., and Kudrass, H., 2013, Increasing chemical weathering in the Himalayan system since the Last Glacial Maximum: Earth and Planetary Science Letters, v. 365, p. 243–252, doi:10.1016/j.epsl.2013.01.038.

McArthur, J.M., Ravenscroft, P., Banerjee, D.M., Milsom, J., Hudson-Edwards, K.A., Sengupta, S., Bristow, C., Sarkar, A., Tonkin, S., and Purohit, R., 2008, How paleosols influence groundwater flow and arsenic pollution: A model from the Bengal Basin and its worldwide implication: Water Resources Research, v. 44, W11411, doi:10.1029/2007WR006552.

McLennan, S.M., 1993, Weathering and global denudation: The Journal of Geology, v. 101, p. 295–303, doi:10.1086/648222.

McLennan, S.M., Bock, B., Hemming, S.R., Hurowitz, J.A., Lev, S.M., and McDaniel, D.K., 2003, The roles of provenance and sedimentary processes in the geochemistry of sedimentary rocks, *in* Lentz, D., ed., Geochemistry of Sediments and Sedimentary Rocks: Evolutionary Considerations to Mineral Deposit-Forming Environments: St. John's, Newfoundland, Geological Association of Canada, GEOtext, v. 4, p. 7–38.

Milliman, J.D., and Syvitski, J.P.M., 1992, Geomorphic/tectonic control of sediment discharge to the ocean: The importance of small mountainous rivers: The Journal of Geology, v. 100, p. 525–544, doi:10.1086/629606.

Morgan, J.P., and McIntire, W.G., 1959, Quaternary geology of the Bengal basin: East Pakistan and India: Geological Society of America Bulletin, v. 70, p. 319–342.

Najman, Y., 2006, The detrital record of orogenesis: A review of approaches and techniques used in the Himalayan sedimentary basin: Earth-Science Reviews, v. 74, p. 1–72.

Nesbitt, H.W., and Young, G.M., 1982, Early Proterozoic climates and plate motions inferred from major element chemistry of lutites: Nature, v. 299, p. 715–717, doi:10.1038/299715a0.

Nesbitt, H.W., Young, G.M., McLennan, S.M., and Keays, R.R., 1996, Effects of chemical weathering and sorting on the petrogenesis of siliciclastic sediments, with implications for provenance studies: The Journal of Geology, v. 104, p. 525–542, doi:10.1086/629850.

Nicholls, R.J., and Goodbred, S.L., 2005, Towards integrated assessment of the Ganges-Brahmaputra delta, *in* Chen, Z., Saito, Y., and Goodbred, S., eds., Megadeltas of Asia: Geological Evolution and Human Impact: Beijing, China Ocean Press, p. 168–181.

Nittrouer, C.A., Austin, J.A., Field, M.E., Kravitz, J.H., Syvitski, J.P.M., and Wiberg, P.L., eds., 2007, Continental Margin Sedimentation: From Sediment Transport to Sequence Stratigraphy: International Association of Sedimentologists Special Publication 37, 560 p.

Pate, R.D., Goodbred, S.L., Jr., and Khan, S.R., 2009, Delta double-stack: Juxtaposed Holocene and Pleistocene sequences from the Bengal basin, Bangladesh: Sedimentary Record, v. 7, no. 3, p. 4–9.

Pickering, J.L., Goodbred, S.L., Reitz, M., Hartzog, T.R., Mondal, D.R., and Hossain, Md.S., 2013, Holocene channel avulsions inferred from the late Quaternary sedimentary record of the Jamuna and Old Brahmaputra River valleys in the upper Bengal delta plain: Geomorphology (in press), doi:10.1016/j.geomorph.2013.09.021.

Prasad, S., and Enzel, Y., 2006, Holocene paleoclimates of India: Quaternary Research, v. 66, p. 442–453, doi:10.1016/j.yqres.2006.05.008.

Rahaman, W., Singh, S.K., Sinha, R., and Tandon, S.K., 2009, Climate control on erosion distribution over the Himalaya during the past ~100 ka: Geology, v. 37, p. 559–562, doi:10.1130/G25425A.1.

Reitz, M.D., Jerolmack, D.J., and Swenson, J.B., 2010, Flooding and flow path selection on alluvial fans and deltas: Geophysical Research Letters, v. 37, L06401, doi:10.1029/2009GL041985.

Richards, A., Parrish, R., Harris, N., Argles, T., and Zhang, L., 2006, Correlation of lithotectonic units across the eastern Himalaya, Bhutan: Geology, v. 34, p. 341–344, doi:10.1130/G22169.1.

Rudnick, R.L., and Gao, S., 2003, Composition of the continental crust, *in* Rudnick, R.L., ed., Treatise on Geochemistry, Volume 3: Amsterdam, Elsevier, p. 1–64.

Sarkar, A., Sengupta, S., McArthur, J.M., Ravenscroft, P., Bera, M.K., Bhushan, R., Samantaa, A., and Agrawal, S., 2009, Evolution of Ganges–Brahmaputra western delta plain: Clues from sedimentology and carbon isotopes: Quaternary Science Reviews, v. 28, p. 2564–2581, doi:10.1016/j.quascirev.2009.05.016.

Schärer, U., Hamet, J., and Allègre, C.J., 1984, The Transhimalaya (Gangdese) plutonism in the Ladakh region: A U-Pb and Rb-Sr study: Earth and Planetary Science Letters, v. 67, p. 327–339, doi:10.1016/0012-821X(84)90172-9.

Singh, M., Singh, I.R., and Müller, G., 2007, Sediment characteristics and transportation dynamics of the Ganga River: Geomorphology, v. 86, p. 144–175, doi:10.1016/j.geomorph.2006.08.011.

Singh, S.K., and France-Lanord, C., 2002, Tracing the distribution of erosion in the Brahmaputra watershed from isotopic compositions of stream sediments: Earth and Planetary Science Letters, v. 6341, p. 1–18.

Singh, S.K., Kumar, A., and France-Lanord, C., 2006, Sr and $^{87}Sr/^{86}Sr$ in waters and sediments of the Brahmaputra River system: Silicate weathering, CO_2 consumption and Sr flux: Chemical Geology, v. 234, p. 308–320, doi:10.1016/j.chemgeo.2006.05.009.

Singh, S.K., Santosh, K.R., and Krishnaswami, S., 2008, Sr and Nd isotopes in river sediments from the Ganga Basin: Sediment provenance and spatial variability in physical erosion: Journal of Geophysical Research, v. 113, F03006, 18 p., doi:10.1029/2007JF000909.

Sinha, R., Tandon, S.K., Gibling, M.R., Bhattacharjee, P.S., and Dasgupta, A.S., 2005, Late Quaternary geology and alluvial stratigraphy of the Ganga basin: Himalayan Geology, v. 26, p. 223–240.

Steckler, M.S., Akhter, S.H., and Seeber, L., 2008, Collision of the Ganges-Brahmaputra delta with the Burma arc: Implications for earthquake hazard: Earth and Planetary Science Letters, v. 273, p. 367–378, doi:10.1016/j.epsl.2008.07.009.

Stewart, R.J., Hallet, B., Zeitler, P.K., Malloy, M.A., Allen, C.M., and Trippett, D., 2008, Brahmaputra sediment flux dominated by highly localized rapid erosion from the easternmost Himalaya: Geology, v. 36, p. 711–714, doi:10.1130/G24890A.1.

Thiede, R.C., Ehlers, T.A., Bookhagen, B., and Strecker, M.R., 2009, Erosional variability along the northwest Himalaya: Journal of Geophysical Research–Earth Surface, v. 114, F01015, doi:10.1029/2008JF001010.

Umitsu, M., 1993, Late Quaternary sedimentary environment and landforms in the Ganges delta: Sedimentary Geology, v. 83, p. 177–186, doi:10.1016/0037-0738(93)90011-S.

Walsh, J.P., Corbett, D.R., Ogston, A.S., Nittrouer, C.A., Kuehl, S.A., Allison, M.A., and Goodbred, S.L., Jr., 2014, Shelf and slope sedimentation associated with large deltaic systems, *in* Bianchi, T.S., Allison, M.A., and Cai, W.-J., eds., Biogeochemical Dynamics at Major River-Coastal Interfaces: New York, Cambridge University Press, p. 86–117.

Wasson, R.J., 2003, A sediment budget for the Ganga-Brahmaputra catchment: Current Science, v. 84, p. 1041–1047.

Weinman, B., Goodbred, S.L., Jr., Zheng, Y., van Geen, A., Aziz, Z., Singhvi, A., and Steckler, M., 2008, Controls of floodplain evolution on shallow aquifer development and the resulting distribution of groundwater arsenic: Araihazar, Bangladesh: Geological Society of America Bulletin, v. 120, p. 1567–1580, doi:10.1130/B26209.1.

Woodroffe, C., Nicholls, R., Saito, Y., Chen, Z., and Goodbred, S.L., 2006, Landscape variability and the response of Asian megadeltas to environmental change, *in* Harvey, N., ed., Global Change and Integrated Coastal Management: Springer, p. 277–314.

Zeitler, P.K., Meltzer, A.S., Koons, P.O., Craw, D., Hallet, B., Chamberlain, C.P., Kidd, W.S.F., Park, S.K., Seeber, L., Bishop, M., and Shroder, J., 2001, Erosion, Himalayan geodynamics, and the geomorphology of metamorphism: GSA Today, v. 11, no. 1, p. 4–9, doi:10.1130/1052-5173(2001)011<0004:EHGATG>2.0.CO;2.

Science Editor: A. Hope Jahren
Associate Editor: Timothy Lawton

Manuscript Received 17 July 2013
Revised Manuscript Received 18 April 2014
Manuscript Accepted 7 May 2014

Printed in the USA